Water Injection Dredging

Advancing Water Injection Dredging: Analysis of Production Rates, Power Requirement, and Dredging Processes

CIEM0500: Thesis

P. J. Prins

Delft University of Technology

TU Delft

Van Oord
Marine ingenuity

Water Injection Dredging

Advancing Water Injection Dredging: Analysis of Production Rates, Power Requirement, and Dredging Processes

by

P. J. Prins

to obtain the degree of Master of Science
at the Delft University of Technology

Student number:	4588118	
Project duration:	March 2024 - December 2024	
Thesis committee:	Prof. dr. ir. M. van Koningsveld	Committee chair, TU Delft
	ir. M. van den Heuvel	Company supervisor, Van Oord
	dr. ir. J.A.A. Antolinez	Committee member, TU Delft
	A. Kirichek	Committee member, TU Delft
	ir. A. Sepehri	Daily supervisor, TU Delft

Cover: Water Injection Dredging vessel 'Maas', located in Rotterdam on August 10, 2024

TU Delft

Van Oord
Marine ingenuity

Preface

The following document represents the findings of the Master's thesis conducted in order to fulfill the requirements of the Hydraulic Engineering programme at the faculty of Civil Engineering and Geosciences of the Delft University of Technology.

This research was done in collaboration with the Delft University of Technology and Van Oord, a marine contractor. My motivation for undertaking this thesis can be traced back to my early interest in soil-water interaction. The world of dredging was revealed to me during my study and inspired me to carry out this research. During the course of this research, I found the working environment at Van Oord to be conducive to my professional development and was grateful for the support I received from its employees, for which I would like to express my gratitude to all who provided me with guidance during this research. I am also particularly grateful to the company for offering students the unique opportunity to gain first-hand experience of a professional work environment.

I would like to express my gratitude to a number of individuals who have provided invaluable assistance and support throughout the process. First is the chair of my committee, Mark van Koningsveld, who inspired me to engage with this research and provided constructive yet incisive feedback. Secondly, I would like to acknowledge my daily supervisor Arash Sepehri, a PhD student and also conducted his research at Van Oord at the same time. Arash was always very kind to me, and I felt that I could always reach out for questions, notes or other inquiries. Without Arash, I would not have improved my academic skills as much and the report would not have reached this level. I would also like to show appreciation to Marcel van der Heuvel, my supervisor at Van Oord. Marcel showed me the operational side of a WID, where the technical and practical fields cross. Marcel always took time out for me, something I really appreciate. He also made sure that I was involved at the WID-days, the christening of the new vessels and made it possible for me to visit a WID during dredging operation, which are moments I will remember. I would also like to give thanks to my remaining committee members, with particular acknowledgment to Alex Kirichek, who facilitated this thesis opportunity, and provided enthusiastic Ports and Waterways and cross-over courses. Finally, appreciation is expressed to my parents, girlfriend and friends, who all had to contend with my complaints, yet consistently provided support and feedback.

Pepijn Prins
Rotterdam, November 2024

Abstract

Climate change has raised awareness of the human impact on the environment, leading to increased global action, including that of the dredging industry. The dredging industry contributes to climate change as dredging and transporting sediments are energy-intensive processes. The International Maritime Organization (IMO) outlines three emission mitigation pathways for the maritime industry, related to design, operational measures, and innovative fuel transition approaches. While design and fuel transition approaches are capital-intensive and time-consuming, implementing operational strategies and gaining a detailed understanding of equipment and processes can help dredging contractors mitigate emissions, and are directly applicable to the dredging fleet. Analyzing the implementation of strategies is done by simulating the dredging processes and estimating the emissions of each process. The potential insights of an emissions estimation model increase the accuracy of emission calculations for dredging contractors and port authorities and help in the testing of potential strategies and their corresponding emissions.

Maintenance dredging is mainly categorized into sediment re-allocation (collecting sediments from one area and discharging them in another location) and sediment remobilization (suspending sediments from the bed to facilitate its transport). The most used vessel for maintenance dredging is a hydraulic Trailing Suction Hopper Dredger (TSHD) for sediment re-allocation. However, a type of dredging equipment that has gained popularity over the years is a Water Injection Dredger (WID), which employs a hydrodynamic dredging technique to re-mobilize the sediment. Water injection dredging utilizes hydrodynamic forces or bed gradients to transport the sediment horizontally after fluidizing the bed, unlike other dredging techniques that physically transport the sediment in a hopper or a pipeline system. This makes a WID a cost and energy-efficient dredging technique, as no additional equipment is needed and the sediments are re-allocated by natural processes.

While considerable research has been conducted on the efficiency and emission of conventional dredging equipment such as TSHDs, relatively little attention has been devoted to WIDs, despite their increased utilization in maintenance dredging projects. As a result, it is currently difficult to compare a work method that is based on the use of a WID, with work methods that are based on conventional dredging vessels. This research aims to address this research gap by developing a model to estimate production rates and power requirement and by simulating WID's processes. This will enable the comparison between a WID-based work method and a TSHD-based work method, which resulted in the following main Research Question:

How can a WID be effectively integrated into a method for comparing the production rates and energy footprints with conventional dredging techniques in port maintenance dredging?

Simulating the processes of maintenance dredging equipment provides a more detailed understanding of project specifications and develops insight into calculating the energy footprint and selecting strategies. Calculating the energy footprint for a dredging vessel is done previously, focusing on their different processes, e.g., loading, unloading, and sailing. The energy footprint calculation is conducted by utilizing a discrete-event simulation package OpenCLSim that facilitates the selection of sustainable strategies and the most efficient setup for the equipment after fleet assignment. To integrate a WID's work methods in OpenCLSim, the tool was modified to facilitate the simulation of a WID, with the development of a novel activity and corresponding attribute. The activity and attribute are used to model the process of remobilization of sediments. Following remobilization, sediments are transported to a High-Energy Environment (HEE) by a WID and returned to the natural system by hydrodynamic forces and bed gradients. This process is simulated in OpenCLSim using the developed activity and attribute to allow the sediment to be removed from the simulation environment.

To simulate the operational process of WID-based maintenance dredging works, the production rate is estimated by empirical and theoretical methods. The empirical-based equations employ an entrainment factor, which quantifies the amount of water that is drawn into the water jet flow as it moves through the water. An additional factor that represents the amount of water needed for fluidization is introduced to estimate the total discharge onto the bed. The theoretical-based equations are based on for the water jets of hydraulic dredging and designed for disintegrating the soil while a WID relies on the process of fluidization. A final method was developed, based on the historical data set of WID-based maintenance dredging works, and incorporates the density, composition, grain size, and plasticity index of the soil to make a context-specific production rate estimate.

To compare WID-based dredging works with conventional-based dredging works, the energy footprint is calculated for each strategy by identifying the main power consumers on a WID: the engine, jet pumps, bow thruster, and board net appliances. For each power consumer, the power requirement is calculated in dedicated modules. With the operational duration of the power consumer, the energy footprint is calculated in OpenCLSim. A case study was utilized to validate estimates of production rate and power requirement. The production rate validation relied on in and out survey data, and the power requirement validation was done by analyzing filtered data extracted from the vessel logs. The effective propulsion power is estimated by first calculating the vessel's resistance and then applying its operational velocity. The metrics of the jet pumps are estimated using an in-house method of Van Oord. The energy footprint of the bow thruster and board net appliances are estimated using a scaling factor concerning the maximum available power.

A comparison of the different estimating methods for the production rate showed that the entrainment factor for the empirical-based equations introduced uncertainty, resulting in an overestimation of the production rate. The theoretical-based equations showed significant overestimation as they are designed for coarse, compacted material. The final method was shown to be the most reliable due to the ability to incorporate multiple parameters. The case study was consequently used for the comparison of a WID and conventional-based work methods, as it allows for simulation with identical soil, hydrodynamic, and site parameters. The simulation demonstrated that a WID was a factor four more energy-efficient per cubic meter of dredged material compared to a TSHD, supported by findings in literature. The project duration for a WID was considerably longer due to the influence of the tidal restrictions and the larger hopper capacity for the TSHD. The emissions of the TSHD were predominantly influenced by the propulsion power, which is attributed to the distance between the dredging and discharge location. The jet pump, as the primary power consumer on a WID, contributes most significantly to its emissions due to its near-constant operation.

In conclusion, the simulations of the case study demonstrated that a comparison between a WID's maintenance operations and a TSHD's maintenance operations is now feasible, as WID-based work methods can be simulated in OpenCLSim. The model may be employed in future research for comparisons with other dredging equipment, to enhance the efficiency of dredging works in terms of their energy footprint. Furthermore, the model can be utilized to calculate the production rate based on energy consumption, in contrast to a production rate based on time. This enables the optimization strategy with a focus on energy consumption. Additionally, it is recommended that this model is employed to gain a visual insight into the energy footprint throughout maintenance dredging projects. This will assist dredging contractors and port authorities in selecting the optimal dredging strategy. Further research on simulating WID-based maintenance dredging should focus on developing a new method to estimate propulsion power, which would improve the model's accuracy. Additionally, applying the production rate estimation method to various case studies could enhance the method's robustness.

Contents

Nomenclature

AIS Automatic Identification System
CEDA Central Dredging Association
CFD Computational Fluid Dynamics
CSD Cutter Suction Dredger
DMF Distillate Marine Fuel
DP Dynamic Positioning
DT Dynamic Tracking
DWT Dead Weight Tonnage
EEDI Energy Efficiency Design Index
EU European Union
GHG Greenhouse gasses
HEE High Energy Environment
IADC International Association of Dredging Companies
IMO International Maritime Organization
IWT Inland Waterway Transport
KPI Key Performance Indicator
LEE Low Energy Environment
MBL Maintained Bed Level
MGO Maritime Gas Oil
OpenCLSim Open Complex Logistics Simulations
SoD Stand off Distance
STEAM Ship Traffic Emissions Assessment Model
TSHD Trailing Suction Hopper Dredger
UKC Under Keel Clearance
WI Water Injection
WID Water Injection Dredger

1

Introduction

1.1. Context

Climate change has raised awareness of the human impact on the environment and has initiated global action. However, climate change is an ongoing battle, with fossil fuel dependency, economic reliance on unsustainable practices, and political inertia slowing progress. It is promising that governments and industries are implementing initiatives to address these challenges. Governments enact stricter policies, and industries are adapting cleaner technologies and innovating to reduce greenhouse gases (GHGs) and other environmental impacts. Similarly in the maritime industry, the International Maritime Organization (IMO) has established a goal of reducing GHG emissions from marine processes with 40% compared to 2008 levels. The goal of emission mitigation includes dredging activities as dredging and transporting the dredged material are energy-intensive processes (Wasim & Nine, 2017).

Approximately 0.6% of the total global shipping emissions are associated with the global dredging fleet (CEDA, 2022). To address emission mitigation in the dredging sector, IMO suggests three pathways related to design, operational measures, and innovative fuel transition approaches (See Figure 1.1). These pathways help dredging contractors understand how equipment and processes can be modified and what alternative strategies can be implemented to achieve the carbon-free goal for dredging activities.

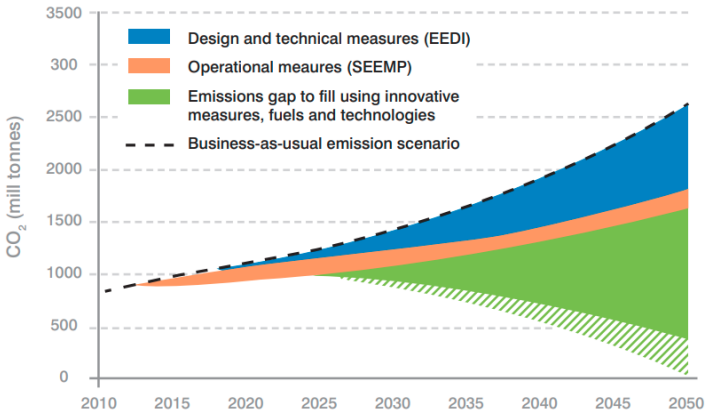

Figure 1.1: Projected CO_2 emissions from maritime shipping under different mitigation strategies. Blue indicates the effect of design and technical measures, orange indicates the operational measures and green indicates the innovative measures, fuel and technologies (Castro et al., 2019).

Implementing different strategies for maintenance dredging and having a detailed understanding of equipment and processes helps in formulating an accurate emission estimation model for the dredging fleet to reduce the energy footprint of dredging works. The potential insights obtained not only increase the awareness of how emission calculations can be done more accurately for both dredging contractors and port authorities but also help them to test possible strategies and measure their emissions.

Dredging can be defined as the process of removing or reallocating sediments from the bottom of water bodies. Dredging activities can be divided into two main categories; with capital dredging, carried out in a new location, the material is dredged for the first time and the soil conditions are predictable. The second category is maintenance dredging, where accumulated sediments are removed periodically to keep existing waterway and port areas at a required water depth, and often heterogeneous soil conditions are present.

Port authorities are responsible for ensuring the safe and navigable passage of vessels within the port. The port accessibility depends on the hydrodynamic conditions, port authority policies, and the fleet characteristics of the vessels calling at the port (Bakker & Van Koningsveld, 2023). The port authorities determine the water level by setting a maintained bed level (MBL), where a deeper MBL increases the accessibility while assuming identical hydrodynamic conditions, but comes with a trade-off to minimize maintenance dredging costs and maximize the port accessibility. To determine the MBL, the method proposed by PIANC (2014) can be used as it provides guidelines to calculate the minimum required Under Keel Clearance (UKC) by accounting for various dynamic factors such as vessel draft, tidal variations, wave action, vessel velocity and seabed conditions. The UKC is defined as the vertical distance between the lowermost point of a vessel and the nearest fixed physical feature underneath the water. This method allows port authorities to set a MBL to accommodate the fleet characteristics of vessels entering a port, ensuring sufficient clearance under varying hydrodynamic conditions. The MBL is established with capital dredging works, maintenance dredging is needed to ensure that the current bed level remains under the MBL.

1.2. Maintenance dredging

Maintenance dredging techniques can be categorized into two main methods; mechanical and hydraulic dredging. Mechanical dredging is the process of removing sediment from the seabed or waterways using mechanical equipment, such as clamshells, buckets, or backhoes. Hydraulic dredging involves the removal of the sediment through suction or pumping systems, where water is mixed with the sediment to create a mixture suitable for removal. As maintenance dredging is frequently conducted on loosely packed and fine sediments, hydraulic methods are often employed for the reallocation of the bulk sediments. Mechanical dredging is often applied for bed levelling details or in locations that are difficult to access.

The most common equipment choice employed for maintenance dredging is a Trailing Suction Hopper Dredger (TSHD) (IADC, 2020). A TSHD utilizes a hydraulic dredging method, where a suction head trails behind the vessel as illustrated in Figure 1.2. The material is transported from the bed into the storage area (hopper) in the vessel. A TSHD is self-propelled and capable of transporting the material horizontally by sailing to the designated discharge location. The material can be released by opening valves in the hopper, transported hydraulically via pipeline sections, or sprayed in an arc shape (rainbowing) onto the desired location.

Figure 1.2: Underwater illustration of a TSHD (Van Oord magazine, 2017)

Instead of relying on hydraulic dredging techniques to reallocate sediments, loosely packed sediments present in port areas are also suitable for remobilization. Remobilization of sediment refers to the process of making the sediment mobile again, after which it can be transported via hydrodynamic currents or bed gradients.

1.3. Water Injection Dredger

An alternative and environmentally friendly approach, which utilizes the remobilization technique for maintenance dredging is a Water Injection Dredger (WID), classified as a hydrodynamic dredging method (IADC, 2013). In contrast to a TSHD, a WID dredges the horizontal transportation of the dredged material occurs in the water column, instead of physical transportation. The next section will discuss the process of a WID in more detail.

The process of a WID consists of three main phases. The first stage is the jetting phase (Figure 1.3A), where large volumes of water under low pressure are injected into the bed by evenly spaced nozzles on a jet beam. The injected water lowers the density of the mud, causing a turbulent, homogeneous layer, which can reach up to 3 meters from the bed (Verhagen, 2000). The second phase of a WID is the transition phase (Figure 1.3B), where a (stable) fluid mud layer is developed. The third phase is the transportation of the fluid mud, driven by gradients, such as gravity, density differences, or hydrodynamic currents (Figure 1.3C). The transportation distance of the fluid mud layer is determined by the settling velocity and the forces driving it.

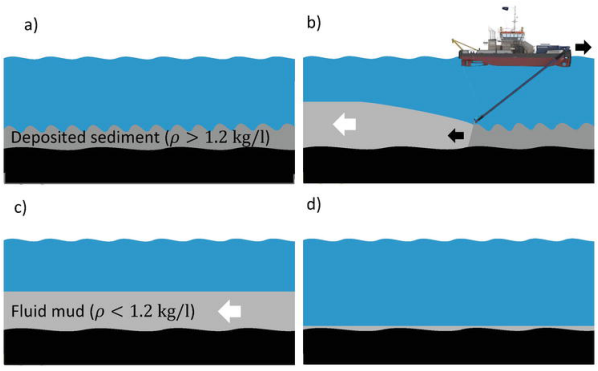

Figure 1.3: Schematized process of a WID on mud. (a) Deposited sediment on the bed; (b) Water if injected onto the bed; (c) A fluidized layer has developed; (d) The fluidized layer is transported by hydrodynamics (Kirichek et al., 2022).

A WID is equipped with one or more jet pumps, which provide the necessary power for the vessel to operate. The vessel operates with injecting water at low pressure, distributed over an array of nozzles via the jet system under low trailing velocities. To prevent sediments of spreading over the area, a WID can extend the horizontal transport distance by fluidizing the same material on multiple occasions. By utilizing a discharge channel, the remobilized sediments are concentrated in a designated area.

A WID is more dependent on local soil conditions than other dredging vessels, local site conditions determine whether fluidization is possible and if the fluidized material can be transported. Additionally, water injection dredging is often only permitted if it has been established that the sediment is not contaminated. When site conditions are favorable, water injection dredging is considered a cost-effective dredging technique as no additional equipment is required, and an energy-efficient dredging technique as it avoids reallocation of sediments (IADC, 2013). The next section goes in-depth into the research conducted on production rates, environmental consequences, and energy footprint of a WID.

1.4. Research background

Maintenance dredging operations are often simulated to gain insight into project details, power requirement, and equipment choices. The production rate, near-field and far-field morphological and environmental consequences of WID works have been investigated in the literature. Winterwerp et al. (2002) investigated the far-field effects of a fluid mud layer, while Spencer et al. (2006) examined the water quality and potential release of toxic metals by the soil after WID operations were conducted. The geomorphic and physicochemical effects of a WID are important to investigate as the consequences can be severe (Pledger et al., 2020). Tyler et al. (2022) looked at the role of hydrodynamics on the production rates of WID. Kirichek and Rutger (2020) monitored a maintenance dredging campaign, where production rates and applicability of a WID were laid out. In this research, a brief comparison with a TSHD is made based on energy consumption. CEDA (2022) compared the specific fuel consumption (how much fuel is needed for one cubic meter of dredged material) of a TSHD and a WID for a maintenance dredging project in the port of Lisbon, where it was concluded that a WID vessel is a factor 10 more fuel-efficient than a TSHD per volume dredged material. However, both studies did not perform an in-depth analysis of the fuel consumption but only calculated the specific fuel consumption with the total amount of fuel used and the total amount of material dredged. An in-depth analysis of the production rate and energy footprint of a TSHD has been done by conducting a simulation tool (Lamers, 2022; Janssen, 2023) but has not been done for a WID.

The dredging industry is implementing methods to reduce their emissions and multiple pathways can be pursued. One mitigation approach is operational measures, where efficiency gains are achieved by enhancing the operational aspects of dredging projects through analysis and optimizing the dredging strategy. The most used dredging vessels for maintenance dredging are TSHDs, which are extensively researched on production rate and emissions estimates. Little research has been conducted on the production rate and emissions for a WID. The missing in-depth power requirement analysis of a WID restricts the possibility of comparing a WID with conventional maintenance dredging techniques. At this moment, there is no method to determine the production rate, power requirement, and emissions in such a way that it also allows it to be compared with other dredging techniques, such as a TSHD. The knowledge gap this thesis aims to fill is the missing in-depth analysis of the production rate and energy footprint of a WID maintenance works, so it can be used.

1.5. Research scope and questions

After identifying the research gap, the research problem and scope are formulated. The research problem is that there is currently no conventional method available to compare dredging techniques with a WID on production and emissions. To address the research problem and fill the existing knowledge gap, this research will quantify the production rate and power requirement of key components of a WID. This research will present a method to compare a WID and a TSHD on key performance indicators (KPI) such as fuel consumption per cubic meter dredged. This will be achieved by integrating modules that quantify the production rate and emissions in a simulation tool, which will then be utilized to analyze and compare a WID with a TSHD.

The tool is used to conduct a simulation of a case study, which is performed with a WID and a TSHD. The results of the simulations are compared to each other and with findings in the literature. The outcomes of this research are designed to improve maintenance dredging operations by optimizing project parameters, the findings should not be used for optimizing vessel parameters. This research focuses on the production rate, power requirement, and emissions of a WID maintenance works, where other environmental impacts of a WID are left out of the scope. The simulation with a TSHD is conducted by utilizing the developed model of previous research.

The main research question is answered by initially addressing the research questions. The main research question is given, after which the research questions are defined.

How can a WID be effectively integrated into a method for comparing the production rates and energy footprints with conventional dredging techniques in port maintenance dredging?

1. What are the key factors and currently used methods for estimating the production rates and energy footprint of a WID?
2. How can a WID be integrated into a currently available method to enable comparison of a WID-based works with conventional based dredging work methods?
3. How can currently unavailable estimating modules for a WID be developed to enable comparison of WID-based work methods with conventional dredging work methods?
4. How can a WID-based work method for port maintenance dredging be compared with conventional maintenance dredging work equipment?

2

Production and Emission

This chapter presents the key factors and methods for estimating the production rate and fuel consumption of a WID. Initially, the production rate is laid out, and subsequently, the methodology to determine the emissions is defined. This chapter concludes with an answer to Research Question 1.

2.1. Production rate background

The key components onboard responsible for the dredging process are the jet pumps and the jet system. The jet system, which consists of two jet pipes and a horizontal jet beam with downward pointed nozzles, pumps large volumes of water with low pressure onto the bed. The efficiency of a WID depends on how much water the vessel is able to inject with its jet system and on how effectively the soil fluidizes. The power of the jet pump, jet system configuration, and sailing velocity determine the discharge on the bed. The standoff distance of the jetbeam to the soil bed and the sailing velocity positively influences the amount of water that is entrained around the water jets, up to a threshold where a limit exists if the impulse of the water jets does not suffice the standoff distance or velocity anymore. The soil conditions determine the response of the soil on the water jets, where the density of the sediment cloud (ρ_{cloud}) is a key parameter of the production rate. Figure 2.1a and 2.1b illustrate the relationship in entrainment and excavation rate, where increased entrainment leads to a greater penetration depth.

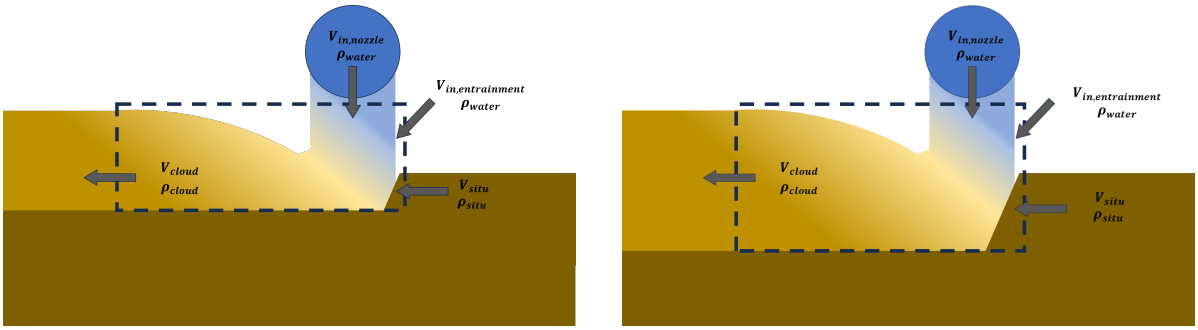

(a) Less entrainment leads to a lower excavation rate

(b) More entrainment leads to a higher excavation rate

Figure 2.1: Comparison of schematic processes for water injection dredging

A WID often operates in a Low-Energy Environment (LEE), where the hydrodynamic conditions do not suffice for the erosion or transport of sediment. The distance between a LEE and a High-Energy Environment (HEE) determines how frequently a WID needs to revisit the same area. When the hydrodynamic parameters or bed gradient are inadequate for sediment to be transported to a HEE, a WID will often dredge a discharge channel, a trench in the bed, towards a HEE. This allows the fluidized material to be collected and prevents it from spreading in the dredging area. An example of a LEE, a discharge channel, and a HEE are shown in Figure 2.2. In practice, this would often be from a sheltered port area to a river or sea.

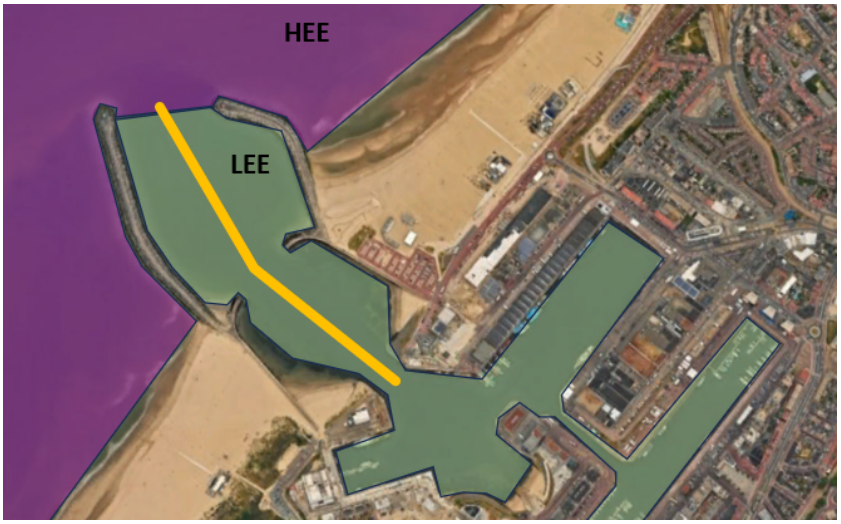

Figure 2.2: Example of Low Energy Environment (green), High Energy Environment (purple), and a discharge channel (yellow) (Google Earth, 2024)

The classification of a LEE and an HEE can be based on the Hjulström graph, shown in Figure 2.3. Hjulström found a relation between the particle grain size, the flow velocity, and the behavior of sediment. The lines in the graph indicate the transition to a different stage for a sediment grain. The distinction between a LEE and an HEE is based on whether a particle can be deposited as bedload. The flow velocities where clay, silt, and sand particles can be transported as bedload are of interest for the process of WID. Using the Hjulström graph can assist in determining the LEE and HEE. If sediment flocs with sizes of 80 μm are present and flow velocities in a LEE are lower than 0.5 cm/s, sediments will deposit. However, it should be noted that this is an indication, as particles of the same material can exist in a range of densities, influencing their behavior.

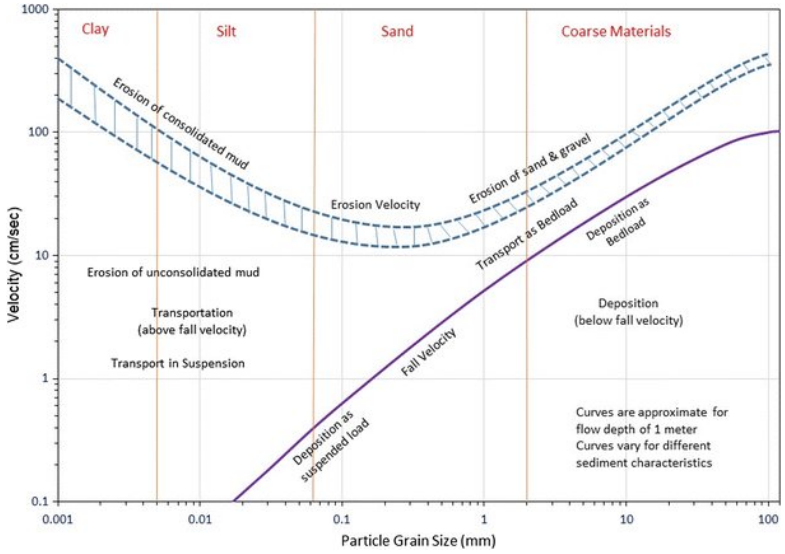

Figure 2.3: Hjulström graph where the areas of deposition, transportation and erosion are depicted for different particle grain sizes (Naganna et al., 2017).

2.2. Excavation rate estimation methods

The calculation of the production rate of a WID is constructed in this research as shown in Figure 2.4. Table 2.1 portraits the parameters used in the estimation of the production rate. The area production (q_{area}), given in Equation 2.1, is the area that can be covered by the vessel per time unit and is determined by the velocity of the vessel during dredging (v_{dredging}) and the width of the jetbeam (W_{jetbeam}).

$$q_{\text{area}} = v_{\text{dredging}} \times W_{\text{jetbeam}} \tag{2.1}$$

The penetration depth of the water jets can be calculated with the area production and the soil parameters. This results in the excavation production, which represents the rate of sediment that is fluidized. However, as a WID relies on hydrodynamics or a bed gradient for horizontal transport, the production rate (amount of material transported to a HEE) is governed by the hydrodynamic parameters.

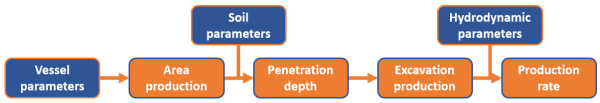

Figure 2.4: General process of estimating the production rate

Table 2.1: Parameters influencing production rate

Vessel parameters	Soil parameters	Hydrodynamic parameters
Jet production	Grain size	Tidal currents
SoD	Situ density	River run-off
Dredging velocity	Shear strength	Distance to HEE
Width jetbar	Porosity	Bed gradients [1]

2.2.1. Survey-based method

The calculation of the production rate of a WID differs from that of a TSHD, as no material is loaded onboard, meaning the amount dredged can not be measured directly. Instead, it is often calculated utilizing in- and out-surveys of the bed, where the bed levels of the surveys are extracted from each other to estimate the total amount of removed material. The moment in time the in and out surveys are conducted has a large impact on the estimation of the production rate. After dredging, continuous siltation occurs, which leads to a lower estimate of the actual production rate. In addition to the timing of the surveys, the surveys also pose uncertainties in validating the estimation of the production rate. Non-intrusive surveys are inaccurate in detecting and monitoring fluid mud layers, as the transition between the water and the fluid mud environment lacks a clearly defined boundary (Draganov et al., 2021).

In literature, the production rate is often calculated with field campaigns where intermittent morphological surveys are done to determine the change of the bed (Kirichek & Rutger, 2020; Pledger et al., 2020; Fuller et al., 2023). Accurately estimating the production rate before a dredging operation is complicated for WID, and no standardized method or equation is found in the literature. Survey-based methods are often applied to validate the dredging works and estimate the production rate afterward.

[1] Although not strictly a hydrodynamic parameter, bed gradients influence horizontal sediment transport.

2.2.2. Empirical-based equation methods

An employed method to estimate the excavation rate, is to derive equations based on empirical data. By deriving equations on empirical data, the estimations method is made accessible for users without the empirical experience. In this research, the empirical-based equations methods are not mentioned due to confidentiality.

2.2.3. Theoretical-based equation methods

Two theoretical methods are presented in this section: the method proposed by Miedema (Miedema, 2019) and in-house handbook method of Van Oord. The first theoretical method was developed for the calculation of the production rate of the water jets in a TSHD (Miedema, 2019). Miedema calculates the production of the draghead by adding the production rates of different components; the high pressure jets production, the draghead production, and the erosion production. A TSHD operates with high pressure jets, so the results are not representative for low pressure jets of WID. However, this method is included for comparison with the other methods. The calculation of the pressure jet production is given below.

The excavation rate of the method by Miedema is given in Equation 2.2, where the area production is multiplied with the penetration depth.

$$Q_{\text{excavation}}^{\text{Miedema}} = q_{\text{area}} \times d_{\text{penetration}} \tag{2.2}$$

The penetration depth is calculated by employing Equation 2.3, which utilizes the Vlasbom coefficient Mass flux (α), the density of the water, a contraction coefficient for the water jets (C_{c}), the area of a nozzle (A_{nozzle}), the water velocity in the jetbeam (u_{jetbeam}) and in the nozzle (u_{nozzle}), the particle density (ρ_{particle}), initial porosity of the soil (n_0) and the dredging velocity.

$$d_{\text{penetration}} = \sqrt{\frac{\alpha \times \rho_{\text{water}} \times C_c \times A_{\text{nozzle}} \times u_{\text{jetbeam}} \times u_{\text{nozzle}}}{\rho_{\text{particle}} \times (1 - n_0) \times v_{\text{dredging}}^2}} \tag{2.3}$$

The velocity of the water at the jetbeam and the nozzle are calculated with Equation 2.4 and 2.5. The pressure drop over the nozzles (with n_{nozzle} the number of nozzles), is calculated with Equation 2.6. The water jet velocity is determined by Bernoulli law. This method assumes that the soil consists of sand and that the water jets fluidize the sand up to the penetration depth.

$$u_{\text{jetbeam}} = \frac{Q_{\text{jet}}}{A_{\text{jet}}} \tag{2.4}$$

$$u_{\text{nozzle}} = \sqrt{\frac{2 \times \Delta p_{\text{nozzle}}}{\rho_{\text{water}}}} \tag{2.5}$$

$$\Delta p_{\text{nozzle}} = \frac{1}{2} \times \rho_{\text{water}} \times \left(\frac{4 \times Q_{\text{jet}}}{C_c \times \pi \times D_{\text{nozzle}}^2 \times n_{\text{nozzle}}} \right)^2 \tag{2.6}$$

Another method that employs theory-based equations, is presented in the handbook of Van Oord. This method is employed for high pressure jets in clay. The method assumes that the SoD is less than six times the water jet diameter, which is a rule of thumb for the impulse of the water jet to reach the bed. Furthermore, this method presents the excavation depth reached by breaking or disintegrating the soil instead of fluidization. The excavation production is calculated with Equation 2.7 with the penetration depth and the area production.

$$Q_{\text{excavation}}^{\text{Handbook}} = q_{\text{area}} \times d_{\text{penetration}} \tag{2.7}$$

The penetration depth is calculated with Equation 2.8, where the nozzle diameter (D_{nozzle}), the pressure in the nozzle (P_{nozzle}), and the undrained shear strength of the sediments (S_{u}) are used.

$$d_{\text{penetration}} = 24 \times D_{\text{nozzle}} \times \frac{\sqrt{P_{\text{nozzle}}}}{\sqrt{S_{\text{u}}}} \tag{2.8}$$

2.2.4. Empirical data method

Besides the empirically derived equations, a method is constructed without formulas, using factors determined by the input parameters, shown in Table 2.2. The density, grain size, and soil composition are used as input, either one or more depending on the availability. The ability to have multiple input parameters helps specify the soil conditions, as a certain soil density can have a range of particle sizes or soil composition. The table is designed to give a more calculated estimation, where the user has insight into the values of other parameters and assists in making a context-specific estimate. The values were designed with soil characteristics present during port maintenance dredging, as heavily compacted soils are not taken into account.

Table 2.2: Production estimates based on different factors **(Note: values are adjusted due to confidentiality)**

Composition:	**Clay [%]**	**Silt [%]**	**Sand [%]**	**Grainsize (D_{50}) [µm]**	**Plasticity Index [-]**	**Density [t/m^3]**	**Penetration thickness [m]**
Clay	40	60	0	2-10	>30	1.25	0.36
Silty clay	30	60	10	10 - 20	30	1.30	0.3233
Clayey sandy silt	20	60	20	20 - 30	20	1.35	0.2867
Sandy clayey silt	10	60	30	30 - 40	10	1.40	0.25
Very sandy silt	0	60	40	40 - 50	<10	1.50	0.2133
Silt - sand	0	50	50	50 - 80	0	1.60	0.1767
Very silty fine sand	0	40	60	80 - 120	0	1.70	0.14
Silty fine sand	0	30	70	120 - 180	0	1.80	0.1033
Fine to medium sand	0	20	80	180 - 250	0	1.90	0.0667
Medium sand	0	10	90	>250	0	2.00	0.03

The layer thickness is used to calculate the excavation rate with the area production, following Equation 2.9.

$$Q_{\text{excavation}}^{\text{factors}} = D_{\text{penetration}} \times q_{\text{area}} \tag{2.9}$$

The final method presented is the earliest production estimate method of a WID, made by Bert Maljers in the 1990s who had over 8 years of experience in the Jetsed, one of the first WIDs. His experience resulted in the Maljer graph, produced for in-house estimates of Van Oord, seen in Figure 2.5. The production rate is plotted against the travel distance for different particle sizes. All lines are plotted for the same operational parameters, and the horizontal transport is based on empirical data or practical experience. Smaller particle sizes have larger transport distances and a clear difference between the muddy sands and the compacted sand. This difference originates in the ability of the soil to be fluidized by the waterjets. With clayey materials, the cohesion between the clay particles is the dominant factor to overcome. With sandy material, particle size and shape are the dominant factors. This results in the difference in production rate between clayey and sandy materials for short transport distances. The transport distance is governed by gravitational force, which is stronger on sand particles due to their large size.

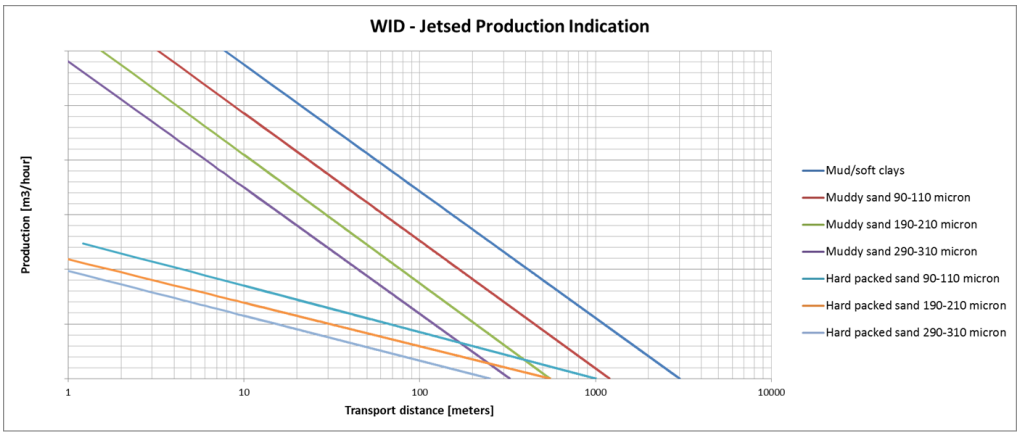

Figure 2.5: Maljers production graph **(Note: axis removed for confidentiality)**

2.2.5. Production rate estimation

Three methods were presented to calculate the excavation rate. To derive at the production rate, the hydrodynamic parameters are used to retrieve the limiting factors. These represent the fraction of the excavation rate that is transported out of the system. The values for the limiting factors due to the tidal amplitude are given in Table 2.3, the factors due to the distance to a HEE are given in Table 2.4. This table should be used with caution, as the factors are not always valid as strong currents are sometimes needed. Equation 2.10 is used to calculate the production rate. This equation can be used with all above mentioned methods to determine the excavation rate.

$$Q_{\text{production}} = Q_{\text{excavation}} \times f_{\text{tidal}} \times f_{\text{distance}} \tag{2.10}$$

Table 2.3: Limiting tidal factors for production rate **(Note: dummy values employed for confidentiality)**

Tidal amplitude	Limiting factor
>5	0.95
4 - 5	0.88
3 - 4	0.79
2 - 3	0.68
1 - 2	0.55
0.5 - 1	0.40
0 - 0.5	0.28
0	0.15

Table 2.4: Limiting distance factors for production rate **(Note: dummy values employed for confidentiality)**

Distance to HEE [m]	Silt / clay	Silt	Sandy silt	Silty fine sand	Medium sand
0 - 50	1.00	1.00	1.00	0.90	0.85
50 - 100	0.95	0.95	0.80	0.72	0.63
100 - 250	0.87	0.87	0.58	0.56	0.41
250 - 500	0.77	0.77	0.39	0.41	0.27
500 - 1,000	0.67	0.67	0.25	0.28	0.17
1,000 - 2,000	0.56	0.56	0.15	0.19	0.10
2,000 - 3,000	0.50	0.50	0.09	0.13	0.05
3,000 - 4,000	0.47	0.47	0.05	0.09	0.03
4,000 - 5,000	0.45	0.45	0.03	0.06	0.02
>5,000	0.45	0.45	0.02	0.05	0.01

2.3. Production estimation comparison

The methods treated in this chapter are used on a base case for comparison. This is done with representative values for the input parameters, given in Table 2.5.

Table 2.5: Base case parameters

Parameter	Value	Unit
ρ_{situ}	1400	kg/m^3
ρ_{cloud}	1070	kg/m^3
ρ_{particle}	2730	kg/m^3
ρ_{water}	1025	kg/m^3
$Q_{\text{jet production}}$	3.0	m^3/s
v_{dredging}	0.514	m/s
SoD	0.4	m
D_{nozzle}	0.090	m
w_{jetbeam}	12	m

Parameter	Value	Unit
A_{tidal}	2.0	m
L_{HEE}	450	m
D_{50}	50	μm
S_{u}	5,000	Pa
C_{c}	0.85	-
n_{nozzle}	41	-
n_0	0.34	-
α	0.1	-

The results of the comparative analysis of the various methods are presented in Figure 2.6. The factors-based method is considered the most robust as it accounts for the greatest number of parameters and is the most recently calibrated method.

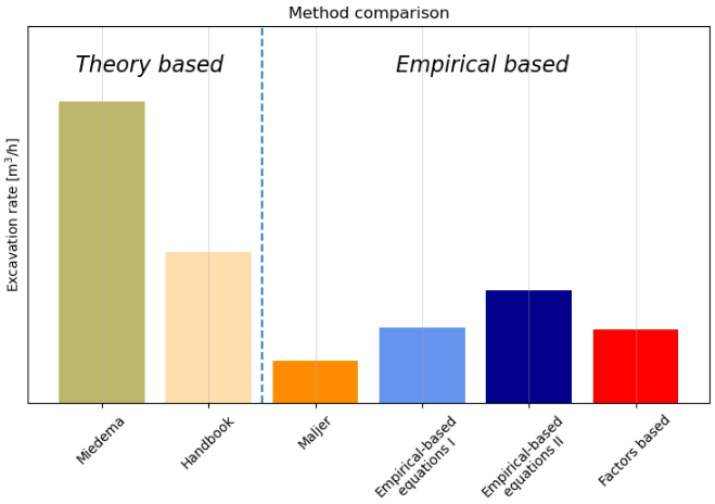

Figure 2.6: Production rate method comparison **(Note: axis removed for confidentiality)**

The methods of Maljer, both empirical-based, and factors-based are derived from historical data. Maljer's method is derived from the historical data of a single WID, the Jetsed. Despite the method accounting for the fewest parameters, the estimation is comparable to that of the factors-based method when the parameters outlined in Table 2.5 are considered.

It can be seen in Figure 2.6 that the theory-based methods yield considerably higher production rate estimates than those obtained through other methods. The two approaches are developed for coarse material, where the shear strength of the soil is provided by the weight of the grains. The methods are designed for disintegrating the soil, rather than fluidization. In contrast, cohesive material, which is often found with maintenance dredging, has smaller particle sizes, with its strength primarily derived from electrostatic forces. As the theory-based methods yield a higher estimation, it can be concluded that the penetration depth of the water jets is overestimated.

The factors-based method has recently been calibrated on historical data, which increases its credibility and accuracy. Soil composition, grain size, plasticity, and density are incorporated into this method, which gives the user a more context-specific estimation. It is consequently regarded as the most accurate representation of the true production rate and is used in this research.

2.4. Emissions background

The emissions calculations are often categorized into two parts, direct and indirect emissions. Direct emissions consist of the emissions produced with the use of the vessel. Indirect emissions originate from the extraction, production, and transportation of the fuel before it is used.

Multiple approaches exist to calculate the direct emissions of a vessel (E_{vessel}), where often the distinction between a top-down and a bottom-up approach is made. The top-down approach does not include the vessel characteristics for calculating the total emissions and is considered unreliable for a single vessel as it only relies on global marine fuel statistics. A bottom-up approach consists of measuring the emissions of a single vessel and extrapolating the results of time and space. This approach can be considered more reliable, but little data is available as this approach is relatively new. The literature often utilizes a combination of the top-down and bottom-up approaches, where the total emissions are calculated (top-down) based on vessel and engine characteristics (bottom-up), and Automatic Identification System (AIS) is used to characterize the emissions in space and time (Ribeiro da Silva et al., 2024). The calculations are often done using a form of Equation 2.11, which can be noted from Appendix A, where multiple methods are laid out. P_{maximum} presents the maximum power installed on the vessel for the primary engine, and f_{load} represents the load factor as a fraction of the maximum installed power capacity. $f_{\text{emissions}}$ is used as a pollutant-specific emission factor. The duration of use of the engine is given as t_{engine} (Merk, 2014).

$$E_{\text{vessel}} = P_{\text{maximum}} \times f_{\text{load}} \times f_{\text{emissions}} \times t_{\text{engine}} \tag{2.11}$$

This research employs a bottom-up approach to estimate the direct emissions generated by a vessel throughout its operational lifetime, as the contribution of the operational phase of a TSHD's lifetime contributes significantly to its overall environmental impact with 99.5 % (CEDA, 2011).

The methodology used for the calculation of emissions is presented in this section. The emissions and fuel consumption are calculated to quantify and compare the results. To retrieve the emissions of a WID, the power requirement is determined for each component and activity. For each component, the mechanical power ($P_{\text{mechanical}}$) is multiplied by the activity duration (t_{activity}) to calculate the energy used using Equation 2.12 for mechanical appliances ($E_{\text{mechanical}}$). Equation 2.13 is used for hydraulic appliances, where the pump pressure (p_{pump}) and the discharge of the pump (Q_{pump}) are used to calculate the energy used ($E_{\text{hydraulic}}$).

$$E_{\text{mechanical}} = \sum_i \left(P^i_{\text{mechanical}} \times t_{\text{activity}}\right) \tag{2.12}$$

$$E_{\text{hydraulic}} = \sum_i \left(p^i_{\text{pump}} \times Q_{\text{pump}}\right) \tag{2.13}$$

The total energy (E_{total}) can be calculated using Equation 2.14, where i represents individual consumers of mechanical and hydraulic power.

$$E_{\text{total}} = \sum_i \left(E^i_{\text{mechanical}}\right) + \sum_i \left(E^i_{\text{hydraulic}}\right) \tag{2.14}$$

The mass of the consumed fuel (m_{fuel}) is determined with Equation 2.15, by employing a Specific Fuel Consumption factor (α_{SFC}). This factor is specific to the type of fuel and represents how much chemical energy is required to produce a given amount of mechanical energy.

$$m_{\text{fuel}} = E_{\text{total}} \times \alpha_{\text{SFC}} \tag{2.15}$$

The amount of CO_2-equivalent emissions (m_{CO_2}) can be determined by using Equation 2.16. The Tank-To-Wheel factor (α_{TTW}) is defined as the amount of emissions produced by burning a kg of fuel from the Tank-To-Wheel (TTW). TTW refers to the emissions produced directly from the combustion of fuel in the engine to when the energy is delivered at the propeller.

$$m_{CO_2} = m_{\text{fuel}} \times \alpha_{\text{TTW}} \tag{2.16}$$

2.5. Production rate and emissions overview

This chapter is used to answer research question 1:

What are the key factors and currently used methods for estimating production rates and energy footprint of a WID?

The key factors for estimating the production rates are categorized into vessel, soil, and hydrodynamic parameters. To determine the production rate of a WID, it is necessary to estimate two uncertain parameters; the entrainment factor and the cloud density. The entrainment factor represents the amount of water that is drawn into the jet flow as the jet stream moves through the water. The cloud density is the density of the fluid mud layer and is governed by the in situ density of the sediment and the amount of water that is injected into the bed. The in situ density of sediment is often heterogeneous with maintenance dredging works, increasing the difficulty of estimating the production rate.

A distinction must be made between the excavation and production rate due to the horizontal transport not being controlled by the vessel, as most methods often calculate the excavation rate. Six methods

were outlined, divided into theory-based methods, empirically derived formulas, and methods derived from empirical data. A factors-based method was developed, which is calibrated on personal experience and historical data of WIDs' maintenance works.

To calculate the emissions produced by a WID's operation, a bottom-up approach is used, where the direct emissions are only considered. The emissions are calculated by a series of equations, where the energy is calculated based on the power requirement and duration of use of a component for mechanical power, and pressure and flow for hydraulic power. Consequently, an SFC and TTW factor are key factors used in the calculations of fuel consumption and emissions.

3

Simulating WID processes

This chapter presents the methodology used to integrate a WID in a tool that allows to compare a WID with conventional maintenance dredging techniques. The employed simulation tool and the adjustments necessary for the purpose of this research are discussed. The frameworks for different phases are given to enable the simulation.

3.1. OpenCLSim

OpenCLSim is an open-source software tool, developed through a collaboration of the TU Delft, Van Oord, Witteveen+Bos, and Deltares. OpenCLSim is used for modeling maritime logistics chains, based on the discrete event simulation package of Simpy (De Boer et al., 2023). OpenCLSim is a discrete deterministic agent-based simulation tool. Although OpenCLSim is an open-source software tool, companies are able to model and define their confidential processes without adding it to the open-source environment, making it attractive for the dredging industry.

This is done previously, where Van Der Bilt (2019) looked into the possibilities of simulating dredging projects to optimize the emissions. A model was developed to quantify the power requirement and emissions so that the user can make a data-driven decision on dredging strategies, based on the input parameters. The full dredging cycle was simulated in OpenCLSim for a typical Dutch coastline reclamation work, to gain an insight into the distribution of power requirement. Lamers (2022) and Janssen (2023) both investigated the power requirement of a TSHD during specific respectively the sailing and loading phases of the dredging cycle. Both employed the same methodology by using OpenCLSim to simulate the dredging activities. The use of OpenCLSim was also employed by De Boer et al. (2023), where it was demonstrated how the model was used to simulate a range of possible barge fleet compositions. This research was built on the work of Baart et al. (2022) and De Boer et al. (2022), where it was shown that OpenCLSim is a suitable tool for simulating processes in the dredging industry. Following the trend in the literature to simulate dredging processes and emissions, a WID is also simulated in OpenCLSim to enable the possibility of comparing dredging equipment.

OpenCLSim is based on the foundation of Simpy, where simulations are based on processes and resources (Matloff, 2008). These processes evolve in time and can be triggered according to a set of given rules. Resources can activate processes and restrict their execution. Combining processes and resources makes Simpy suitable to model scenarios where activities depend on shared resources and compete for their access.

An example of triggered processes for the maritime industry is the installation of a windmill, with the installation process as an activity. The installation vessel is a resource, with the windmill modeled as an object. The installation activity is then triggered when the installation vessel, loaded with the windmill, has arrived at the site. By establishing rules and dependencies in OpenCLSim, maritime processes can effectively be simulated.

OpenCLSim makes use of two main components, the Core module and the Model module. These modules contain the classes and functions. In OpenCLSim, different resources interact with each other according to a set of given rules. To define a resource, OpenCLSim utilizes mixin classes. These are a set of mixin configurations originating from the Core module. More information about the mixin

types can be found in Van Koningsveld et al. (2019). An example of how different mixins are used to simulate a TSHD is given in Table 3.1.

Table 3.1: TSHD mixin configuration example

Mixin	***Explanation***
Locatable	object has a certain position
Movable	object is able to move
Processor	object is able to process objects by dredging
HasContainer	object is able to store an amount in its hopper
HasResource	object is modelled as a Simpy Resource

Dredging activities in OpenCLSim are predefined. In Table 3.2, the activities to perform a TSHD cycle are given: sailing empty, dredging, sailing full, and discharge. With OpenCLSim, the sailing empty and sailing full phases are modeled with the move activity. The dredging and discharge phases are modeled with the shift amount activity. With these operations, a complicated dredging operation is easily modelled. More activities exist in OpenCLSim, providing options to execute activities parallel, while, sequential, or repetitive. This allows the user to set the rules which are needed to schematize the real-world environment.

Table 3.2: Dredging activities example

Activity	***Explanation***	***Requirements***
Move activity	Sailing full and Sailing empty phases	1) Origin 2) Destination
Shift amount activity	Dredging and Discharge phases	1) Origin 2) Destination 3) Processor

OpenCLSim allows the use of plugins. In line with the modular structure of OpenCLSim, plugins are self-defined modules. An example of an open-source plugin is the weather plugin. The plugin can then be used to analyze what the effect on the project is with different types of weather conditions. In previous research, an energy plugin is employed (Lamers, 2022). The plugin is called for each activity, which registers the duration and the power requirement of each component, allowing it to calculate the energy consumption for different components throughout the project.

3.2. Simulating a WID in OpenCLSim

OpenCLSim has been developed for simulating repetitive maritime activities, such as a TSHD cycle within dredging operations. A WID's operation does not follow the same dredging cycles as a TSHD. Figure 3.1a and 3.1b illustrate the dredging cycles of a TSHD and a WID, respectively. The blue boxes and orange arrows represent the activities and the route of the vessel. The green arrows represent the journey of the sediments, whereby the sediment is transported from the dredging location to the discharge location with TSHD. In the case of a WID, the sediment is transported out of the system boundaries by remobilizing the sediment, without control of the destination.

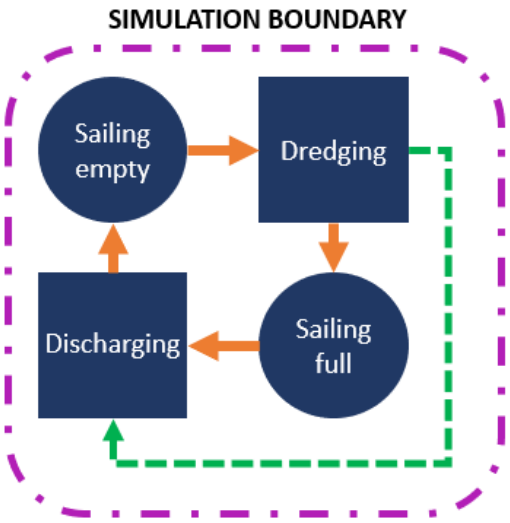

(a) Schematized dredging cycle of a TSHD

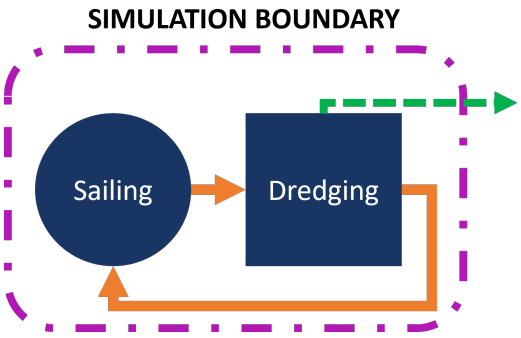

(b) Schematized dredging cycle of a WID

Figure 3.1: Schematized system boundaries and dredging cycles for TSHD and WID, where blue areas represent the activities, green arrow shows the sediment pathway, and purple represent the simulation environment.

Table 3.3 highlights the difference between a standard TSHD's cycle and a WID's dredging cycle. The key difference with a WID is the dredging and discharge phase, where a WID does not handle sediment. To simulate this process in OpenCLSim, additions to the Core module and the Model module are needed. The Core module allows the user to give properties to an object. The model module allows the user to define the activities.

Table 3.3: Dredging phases overview

TSHD's cycle phases	*WID's cycle phases*	*Remarks*
Sailing empty	Sailing to project location	Only occurs once in a project
Dredging	Producing	No sediment is dredged, but remobilized
Sailing full	N.A.	WID does not transport the sediment
Discharge	N.A.	Discharge location is determined by hydro-dynamic forces
N.A.	Waiting	Utilized when a tidal window is in place

3.2.1. Model module

To accurately model an operation of a WID in OpenCLSim, the Shift Amount activity cannot be used. As seen in Table 3.2, the Shift amount activity requires that a destination for the sediment is defined. With WID, the sediment is moved by hydro-dynamic forces which results in an unknown location. In an ideal project case for a WID, the sediment is relocated to a HEE, resulting in its disappearance from the model environment. This eliminates the possibility of defining a destination for the sediment.

In order to overcome this limitation, a new activity is created called the 'Produce Amount Activity', as described in the code repository (Prins, 2024). This activity has three functions. The activity verifies the availability of objects (sediment) in the origin (project location). Secondly, it determines if a WID (resource) is available. Finally, the objects are released from the origin, but the destination location will not register the objects. This results in the disappearance of sediment, as the origin resource releases the objects and does not register elsewhere.

In the Produce Amount Activity, it is necessary to define an amount and a duration as input parameters. This is done through the use of an external Python script, for three purposes. The first reason for this approach is that the determination of the WID's production rates and duration can be confidential. By defining the production rate and duration in an external script, the Produce Amount Activity can be made publicly accessible, while users can still use their confidential calculations. The second reason

for this approach is that the determination of production rates involves significant uncertainty. Segregating these uncertainties into separate modules makes it possible to update them in the future without adjusting the Core- and Model modules of OpenCLSim. The final reason to model the activity in this manner is to be consistent with the other activities of the Model module of OpenCLSim.

3.2.2. Core module

As mentioned in the preceding paragraph, a new activity was required for the simulation of the sediment process during WID. However, the activity must be performed by a processor, as indicated in Table 3.2. The processor mixin is predefined in the Core module of OpenCLSim and in order to shift the amount, the processor performs checks on whether the material is located in the origin and is possible to be located at the destination. As this will not be the case with WID, a new processor was developed for WID, described in the code repository (Prins, 2024).

The changes made to the core and model module are summarized below in Table 3.4. The WID processor is specifically made for the Produce Amount Activity. With the original processor mixin, checks are done to ensure that it is possible to shift an amount. The WID processor mixin doesn't perform these checks, but it does handle the amount. This is necessary for registering the amount of sediment that has been remobilized by the WID.

Table 3.4: Adjusted modules for a WID

Module	Mixin	Conventional	WID
Core	Processor	1) Checks the availability in the origin	1) Checks the availability in the origin
		2) Checks the availability in the destination	2) Renamed to: WIDprocessor
Model	ShiftAmountActivity	1) Releases objects from the origin	1) Releases objects from the origin
		2) Registers objects at the destination	2) Renamed to: ProduceAmountActivity

3.2.3. OpenCLSim plugins

While simulating a WID in OpenCLSim, the energy consumption is calculated with a plugin. The energy plugin generates a list where the power and duration of each component of the vessel is given, sorted per activity. The energy plugin is activated with each activity, calculating the required power and multiplying it with the time used, resulting in an energy consumption per component. An overview of which component is calculated during moving, dredging, or preparation phase is given in Table 3.5.

Table 3.5: Power consumers per activity

Activity	Propulsion	Jet pumps	Bow thrusters	Board net
Sailing	x		x	x
Dredging	x	x	x	x
Preparation				x

Dredging vessels operate in a window of hydrodynamic conditions wherein dredging operations can be conducted by the vessel. The presence of strong winds and waves can impede the vessel's maneuverability or damage the dredging equipment. In the context of WID, the operational window is not only determined by winds and waves but also by tide. A WID makes use of the hydrodynamic conditions to transport the sediment, with often the tide being the primary transport mechanism. To implement this in OpenCLSim, a tidal plugin was made, used when a dredging activity is called in the simulation. If the dredging activity is initialized, the tidal plugin checks whether an outgoing tide is present. If not, the dredging plugin delays the activity. As soon as the outgoing tide starts, the dredging activity is also allowed to start and initialize. The tidal plugin can be customized to have water depth as a threshold, as well as moving the dredging window in time. In cases where the water depth is insufficient for the vessel to reach the area, the water depth is set as a threshold. Figure 3.2 shows an example of a dredging window based on the incoming and outgoing tide. When an outgoing tide is present, negative water velocities are present. The green planes indicate when dredging is allowed to start. The negative

water velocities allow the sediment to be transported to a HEE. The tidal window determines when the dredging activity starts, and when the dredging activity ends.

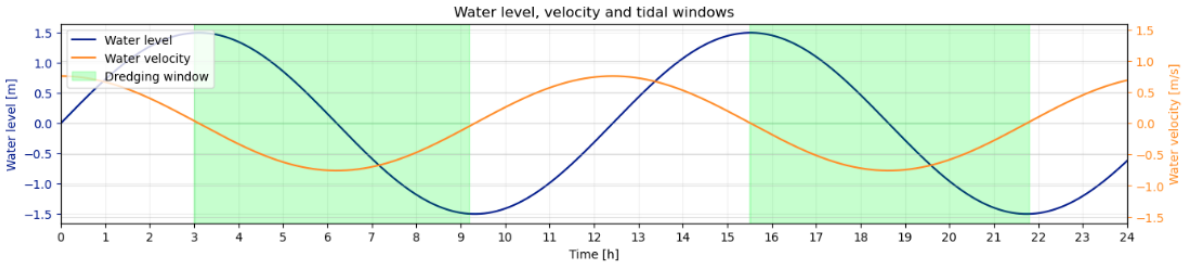

Figure 3.2: Example of tidal plugin dredging windows in green, water level in blue and velocity in orange

This section explains the framework used to simulate a WID's project. As explained in previous sections, the WID's operation is modeled with three different phases: the sailing phase, the dredging phase, and the preparation phase. The sailing phase of a WID's operation is comparable to the already predefined move activity of OpenCLSim. This implements the energy plugin during moving relatively straight forward and is proven to be reliable (Van Der Bilt, 2019). The workflow used is depicted in Figure 3.3. The green boxes represent the input parameters. The blue boxes are external modules, that perform calculations. The inputs and outputs are represented by the orange arrows and boxes.

3.2.4. Sailing phase

The sailing phase is either applied when a WID is sailing to or from its project location. The velocity with respect to the ground is given as project input, and utilized to calculate the hull resistance. The propeller power dependents on the resistance force and velocity. The onboard power and bow thruster power are added. The power is multiplied by the duration of the sailing phase, resulting in the total energy consumed during the activity.

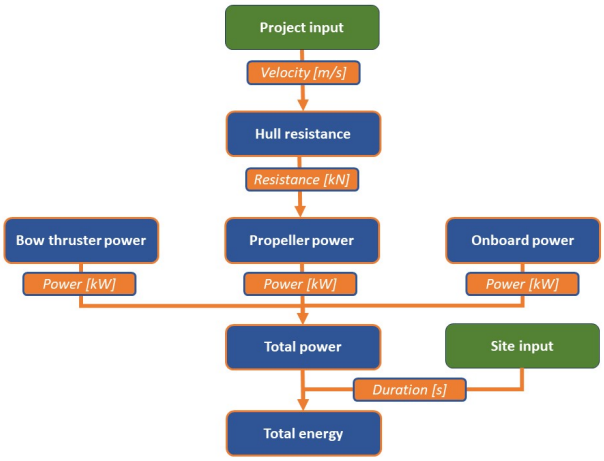

Figure 3.3: Schematic overview of power requirement during sailing phase

3.2.5. Dredging phase

The dredging phase is initialized when the jet beam is lowered. A WID sails back and forth, making a zigzag pattern to cover the working area. This movement is modeled as a straight line, where a factor α will simulate the time the bow thrusters are in use for sideways displacement. OpenCLSim is a discrete-event simulation, the actual movement of the vessel does not need to be simulated in detail as the focus is on modeling the sequence of events rather than continuously simulating each moment in time.

The dredging phase of a WID's operation is schematized in Figure 3.4. The schematization of the

dredging phase is extended compared with the sailing phase, by adding the jetbeam resistance and the jet pump power. The jet beam resistance is, similar to the hull resistance, dependent on the velocity of the vessel during dredging. The hull resistance and the jet beam resistance are added together to determine the required propeller power. The total power requirement during the dredging phase is determined by an extra element, the jet pumps. The jet pump power requirement input parameters are the pump characteristics, the required flow, and the jet pump speed.

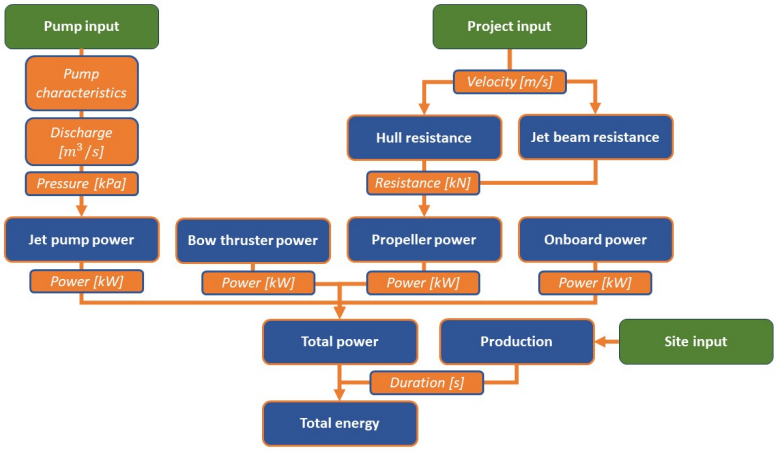

Figure 3.4: Schematic overview of power requirement during dredging phase

During the dredging phase, there is a need to distinguish the operational hours from the total time. The operational hours of the project are used to determine the production. The total dredging time, excluding the operational delays, external delays, technical delays, and out-of-service time results in the operational hours. The main cause of external delays is vessel traffic, operational delay is attributed to the turning of the vessel and other causes of discontinuity during the dredging phase.

3.3. WID simulation overview

This chapter presented the methodology used to simulate a WID and answered Research Question 2:

How can a WID be integrated into a currently available method to enable the comparison of a WID-based works with conventional based dredging work methods?

Previous research has demonstrated that OpenCLSim is a currently available simulation tool that is proven to be suitable for simulating cyclic marine activities and has an agent-based discrete event framework. However, adjustments are made to OpenCLSim to account for the hydrodynamic remobilizing technique of WID. These adaptations have been made by developing a tidal plugin, a new activity, and an accompanying WID processor, where the WID processor is able to release sediments from its simulation environment with the new activity without specifying a new location. This enabled the integration of the WID functionality into the existing OpenCLSim tool, with the associated code available in the repository (Prins, 2024).

It was further shown how the production rate and energy footprint will be integrated into OpenCLSim by using specific frameworks for the different phases of a maintenance dredging operation. Finally, an energy plugin is used to calculate the power requirement and a tidal plugin was developed to simulate the working process of a WID. The estimation of the production rate and energy footprint of different components is detailed in Chapter 4.

4

Simulation modules

This chapter presents the methodology used to construct or adapt the modules necessary to quantify the power requirement of a WID in OpenCLSim. To quantify and integrate the power requirement of a WID's components, the separate modules are developed inline with the framework presented in Chapter 3.

4.1. Propulsion module

The propeller provides the propulsion of a vessel, which is driven by the engine. The power requirement of dredging vessels is, compared to cargo vessels, poorly researched. Previous master theses have investigated the energy consumption of a TSHD during sailing and loading phases (Lamers, 2022; Janssen, 2023), using the method of Holtrop and Mennen. These studies have demonstrated the accuracy of this method for describing the power requirement for the propulsion of a dredging vessel.

One of the most common approaches to determining the required propulsion power for cargo vessels is the Holtrop and Mennen method. However, other prominent methods are outlined in appendix A. The method proposed by Holtrop and Mennen calculates the resistance of the vessel. This is done based on the vessel dimensions, the dimensions of the waterway, and the sailing velocity. Once the total resistance is known, the corresponding propeller power can be calculated. The Holtrop and Mennen method consists of six different resistance elements, which are treated separately in the sections below (Holtrop & Mennen, 1982).

The Holtrop and Mennen method does not consider the impact of shallow water effects. The method is designed for cargo vessels, which typically operate in deep water, and thus no need to incorporate the shallow water effects. Dredging vessels spend a considerable amount of time in shallow water, causing the shallow water effects to be significant enough to be taken into account. When the vessel operates in shallow water, a low-pressure area is created under the vessel, as seen in Figure 4.1.

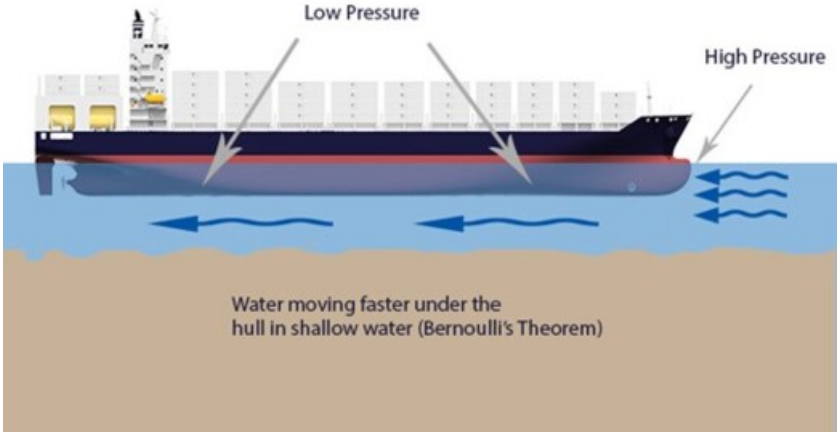

Figure 4.1: Schematized shallow water effect (MySeaTime, 2024)

When operating in shallow water, velocities are often low, resulting in low Froude numbers causing the viscous resistance of the hull of the vessel to significantly increase. The shallow water effects are incorporated using the method of Zeng et al. (2019), who calculates the critical Froude number, based on velocity and water depth. By using a velocity factor, the shallow water effect is accounted for.

The total resistance of a vessel is given in Equation 4.1.

$$R_{\text{total}} = R_F(1 + k_1) + R_{\text{APP}} + R_{\text{W}} + R_{\text{B}} + R_{\text{TR}} + R_{\text{A}} \tag{4.1}$$

Where:

R_{total} = Frictional resistance according to the ITTC-1957 equation $[kN]$
$1 + k_1$ = Form factor describing the viscous resistance of the hull form in relation to $R_F[-]$
R_{app} = Resistance of appendages $[kN]$
R_{W} = Wave-making and wave-breaking resistance $[kN]$
R_{B} = Additional pressure resistance of bulbous bow near the water surface $[kN]$
R_{TR} = Additional pressure resistance of immersed transom stern $[kN]$
R_{A} = Model-ship correlation resistance $[kN]$

The first term of Equation 4.1 describes the resistance caused by friction. The form factor $1+K_1$ includes the viscous resistance. This form factor is based on a large quantity of available historic vessel data.

The appendage resistance includes all appendages on a vessel: rudders, propellers, or bow thrusters. The issue of appendage resistance was not addressed in the model test upon which the method was based, as scaling laws are not applicable in this context. According to Rawson and Tupper (2001), appendage resistance is usually small of the order of 10 percent. This has led to taking the appendage resistance as 10% of the total wetted perimeter for this research.

The wave-making and wave-breaking resistance is only taken into account during the sailing phase. This is done for three reasons. During WID's projects, dredging occurs in sheltered port areas where wave amplitudes are low. When waves are sideways on the WID, the displacement of the jet system is strengthened compared to the vessel itself. The velocity while dredging, 1 knot, is not high enough to experience a significant resistance. The resistance due to the bulbous bow is not taken into account for WIDs, as no bulbous bow is present. This is also the case for the immersed transom stern resistance (Lamers, 2022). The discrepancy between the real world and the model is accounted for by the model-ship correlation resistance.

To calculate the propulsion power ($P_{\text{propulsion}}$), Equation 4.2 is used. With this equation, it is assumed that the vessel has a constant velocity (v_{vessel}) and a constant resistance (R_{total}). The efficiency terms

($\eta_{\text{efficiency}}$) are constructed out of different components, given in Equation 4.3. The values are based on in-house literature of Van Oord.

$$P_{\text{propulsion}} = \frac{R_{\text{total}} \times v_{\text{vessel}}}{\eta_{\text{efficiency}}} \tag{4.2}$$

$$\eta_{\text{efficiency}} = \eta_{\text{open water}} \times \eta_{\text{transmission}} \times \eta_{\text{hydrodynamic}} \tag{4.3}$$

During the production phase of a WID project, an additional resistance factor caused by the jet beam structure is present. A schematization of the jet beam structure is given in Figure 4.2. In this schematization, two drag forces are apparent: the drag forces caused by the jet beam and the drag force caused by the jet pipe. The methodology outlined for estimating the trailing forces of a draghead of a TSHD is applied to estimate the trailing forces of the jet system (Ter Meulen, 2018).

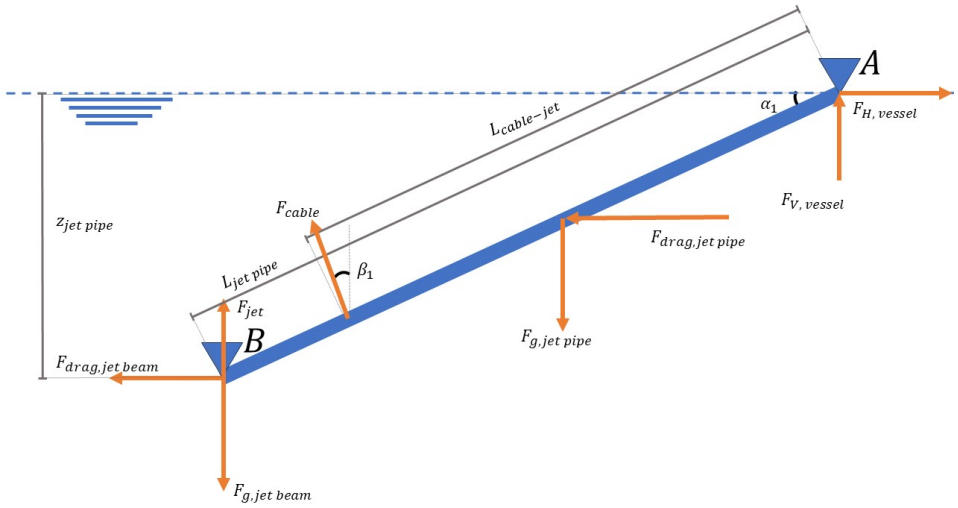

Figure 4.2: Free body diagram of jet system

An immersed body experiences drag due to the flow of water passing by, the flow velocity (v_f). The flow velocity is determined by the velocity of the vessel (v_{vessel}) and the velocity of the fluid (v_{fluid}). These components can reinforce and weaken each other, based on the direction.

The total drag consists of the form drag and the skin friction. More friction terms are present, but it is chosen to exclude them for this research as they are negligible (Granville, 1976). The form drag is aimed perpendicular, while the skin friction is parallel to the jet pipe, seen in Figure 4.3. These drag force components are in the same direction as the jet beam. The drag force is given in Equation 4.4.

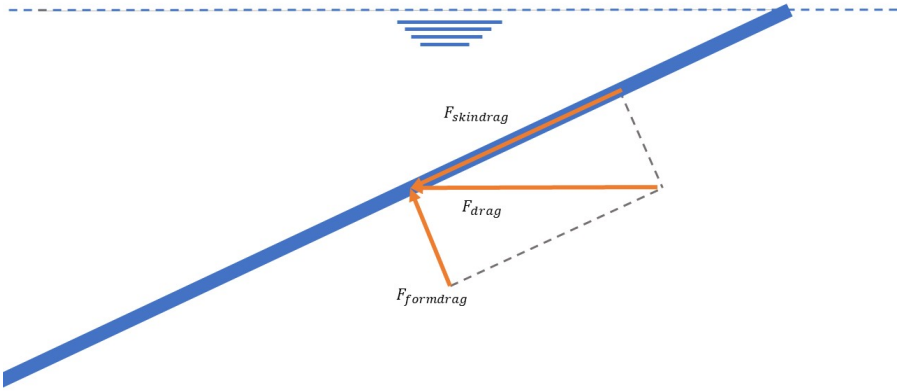

Figure 4.3: Schematic overview of drag force on jet pipe

$$F_{\text{drag}} = \frac{1}{2} \times \rho_{\text{w}} \times C_{\text{d}} \times A_{\text{frontal}} \times v_{\text{f}}^2 \tag{4.4}$$

Where:

F_{drag} = Drag force $[N]$
ρ_{w} = Density of water $[kg/m^3]$
C_{d} = Drag coefficient $[-]$
A_{frontal} = Frontal area of the object $[m^2]$
v_{f} = Flow velocity $[m/s]$

The form drag is determined by the shape of the object. When a fluid comes into contact with an object, a pressure difference is created due to the shape form. A high-pressure area develops in front of the object, while a low-pressure area is created behind the object. The pressure difference over the object results in a force directed against the fluid, resulting in the form drag. The drag coefficient is dependent on the Reynolds number. According to Sadraey (2009), for laminar flow conditions a circular rod has a drag coefficient of 1.2, while for turbulent flow conditions, a circular rod has a drag coefficient of 0.3.

Reynolds numbers are used to describe flow conditions, which in turn determine the drag coefficient. The equation for the Reynolds number is given Equation 4.5. The Reynolds number is the ratio between the fluid's momentum force to the viscous shear force. Low Reynolds numbers indicate laminar flow, while high Reynolds numbers indicate a turbulent flow. The drag coefficient of Equation 4.4 is inversely proportional to the Reynolds number, meaning that lower Reynolds numbers result in higher drag coefficients (Ujile, 2014).

$$R_{\text{e}} = \frac{v_{\text{f}} \times L_{\text{char}}}{\nu} \tag{4.5}$$

Where:

R_{e} = Reynolds number $[-]$
v_{f} = Flow velocity $[m/s]$
L_{char} = Characteristic length $[m]$
ν = Kinematic viscosity $[m^2/s]$

The skin friction is caused by the shearing of the fluid against the object. The resistance to this shearing is determined by the Reynolds number. When a laminar layer develops, the shearing effect will increase. When a turbulent layer develops, the shearing effect will decrease. For a smooth cylinder, a laminar flow regime is present with Reynolds numbers up to 300,000. After the laminar flow regime, the flow regime is in a transitional regime for Reynolds numbers to 3,000,000.

For both the skin and the form drag, the drag coefficient will decrease with increasing Reynolds numbers, as long as the flow regime does not change. As seen in Figure 4.4, a sharp drop-off of the drag coefficient is observed for a sphere around Reynolds numbers of 10^5.

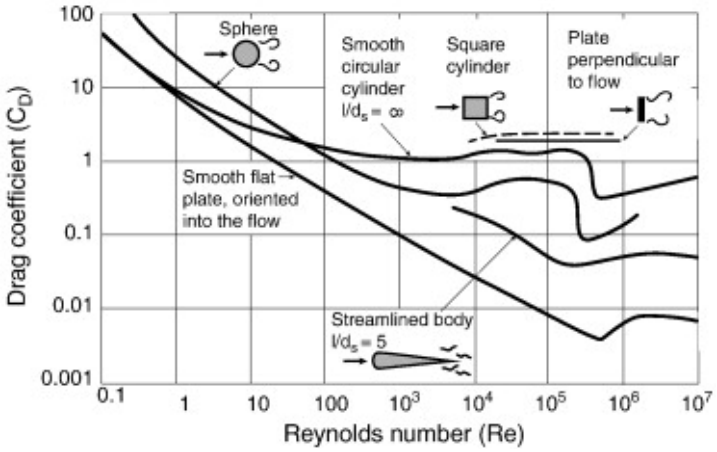

Figure 4.4: Drag coefficients for different Reynolds numbers

With the drag forces now known, an adjustment to Equation 4.1 can be done. The drag forces are an extra resistance term, $R_{\text{jet structure}}$, which is added resulting in Equation 4.6, the equation to calculate the propeller power during dredging.

$$R_{\text{total, dredging}} = R_F(1 + k_1) + R_{\text{APP}} + R_{\text{W}} + R_{\text{B}} + R_{\text{TR}} + R_{\text{A}} + R_{\text{jet structure}} \tag{4.6}$$

For the submerged jet structure, the Reynolds numbers are calculated for the jet beam and the jet pipe. Results are shown with a flow velocity of 1 knots. This is the minimal flow velocity over the jet structure, resulting in the lowest Reynolds number. The minimal Reynolds number is in the highest interest, as the flow regime is expected to be turbulent. Lower Reynolds numbers are associated with the transition regime, which increases the drag coefficient. For the jet pipe, the flow is multiplied with the cosines of α_1, as the perpendicular flow vector is needed. This is done for the maximum angle of 53°, corresponding to a maximum dredging depth of 24 meters, and the minimum angle of 3.8°, corresponding to a minimum dredging depth of 2.1 meters. The length of the jet pipe is 30 meters. The kinematic viscosity is $1 \times 10^{-6}\ m^2/s$ for water with a temperature of 20 °C.

Table 4.1: Reynolds number for jet beam and jet pipe

Structure	*Angle to flow [°]*	*Flow velocity [m/s]*	*Characteristic length [m]*	*Kinematic viscosity [m^2/s]*	Reynolds number [-]
Jet beam	1	0.514	0.81	1×10^{-6}	**438,210**
Jet pipe, form drag	53.13	0.411	0.81	1×10^{-6}	**350,568**
Jet pipe, form drag	4.02	0.036	0.81	1×10^{-6}	**29,187**
Jet pipe, skin friction	53.13	0.308	30	1×10^{-6}	**9,252,022**
Jet pipe, skin friction	4.02	0.512	30	1×10^{-6}	**15,382,061**

The results in Table 4.1 show that the jet pipe has very high Reynolds numbers for skin friction, resulting in negligible skin friction. The form drag of the jet pipe and the jet beam is taken into account. The form drag coefficients are given below in Table 4.2. A drag coefficient of 0.9 is used for the whole jet system. This allows the calculation of the total drag force of the jet system during the dredging phase.

Table 4.2: Drag coefficients

Structure	Drag coefficient [-]
Jet beam	0.8
Jet pipe, form drag (min)	0.8
Jet pipe, form drag (max)	0.7

4.2. Pump module

The jet pumps onboard a WID are crucial equipment. These jet pumps are designed to deliver high discharge under low pressure. According to Van Rijn, L.C. (2012), the jet pumps should be able to deliver a minimum of 1-2 m^3/s of flow rate, with velocities of at least 5 to 10 m/s. Conventional dredging vessels like a TSHD often have multiple pumps; an underwater pump, a jet pump, and a possible booster pump. These pumps experience greater loads as the dredging depth is often deeper, and pumping a slurry requires more power than pumping water. However, it is decided to calculate the power requirement of the jet pumps as a separate module, as dredging operations for a WID are continuous for long hours.

$$P_{\text{pump}} = \Delta p_{\text{pump}} \times Q_{\text{pump}} \tag{4.7}$$

$$E_{\text{pump}} = \int P_{\text{pump}} \times dt \tag{4.8}$$

Where:

P_{pump} = power requirement of pump $[W]$
p_{pump} = Pressure difference over pump $[Pa]$
Q_{pump} = Discharge point of pump $[m^3/s]$

The energy consumption of a pump is calculated by Equation 4.7. The pressure and discharge points are determined by the two factors, the pump curve and the resistance curve, as shown in Figure 4.5. The pump curve is determined by the characteristics of the pump, while the system curve is given by the static head and the friction head. The total head is determined by the properties of the jetpipe, the nozzles, and the dredging depth.

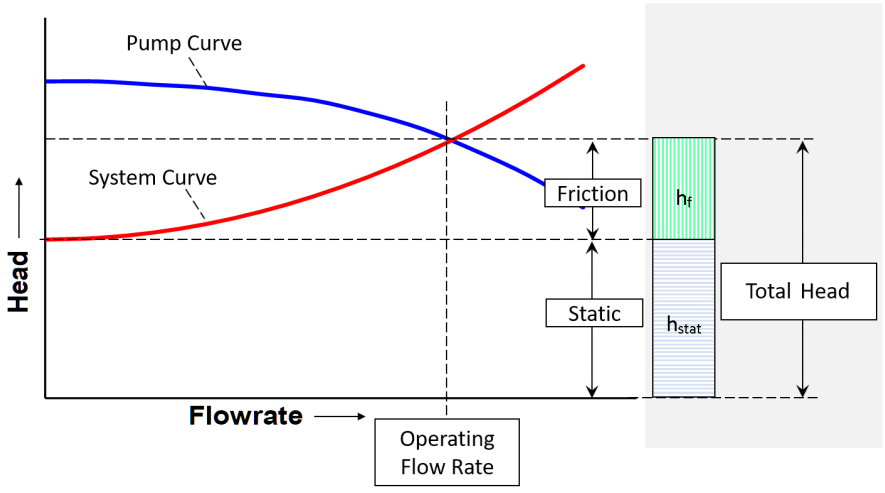

Figure 4.5: Pump and resistance curves (Dahl & Felix, 2020)

The point where the pump and system curves meet is called the working point of the pump. The working point determines the head and flow. Both curves can be adjusted to achieve a desired working point

within the pump's capabilities. By reducing the diameter of the nozzles, the system curve will move up. This results in a working point shifting to the left: a decrease in flow rate and an increase in pressure. To change the pump curve, the operator can reduce or increase the revolutions per minute (RPM) of the pump. Reducing the RPM results in lowering the pump curve, resulting in a shift of the working point to the left.

The pump calculations are performed in a separate module within the model where the input for the calculations is the RPM, as the captain of the vessel alters the RPM to control the pump as well in real life. The pump curve is calculated based on affinity rules, given in Equation 4.9, which describe the relationship of a change in pump speed to the change in flow, pressure, and power (Simpson & Marchi, 2013). When Q_1, H_2, and P_1 are known, affinity laws enable the calculation of Q_2, H_2, and P_2.

$$\frac{Q_1}{Q_2} = \frac{N_1}{N_2} \tag{4.9}$$

$$\frac{H_1}{H_2} = \left(\frac{N_1}{N_2}\right)^2 \tag{4.10}$$

$$\frac{P_1}{P_2} = \left(\frac{N_1}{N_2}\right)^3 \tag{4.11}$$

Where:

$Q =$ Flow rate $[m3/s]$
$H =$ Pressure head $[kPa]$
$P =$ power requirement $[kW]$
$N =$ Rotations per minute $[RPM]$

The resistance curve is calculated by dividing the total resistance into four terms; the pipeline, vacuum, static, and additional resistance, seen in Equation 4.12 to 4.16 (Van Oord, 2023). The pipeline resistance results from the shearing of the water against the pipeline. The vacuum resistance originates in the suction pressure. The static resistance depends on the depth of dredging, and the additional resistance is present due to the bends, valves, and nozzles in the system.

$$R_{\text{pipeline}} = \lambda \left(\frac{L_{\text{pipeline}}}{d_{\text{pipe}}}\right) \times 0.5 \times \rho_{\text{water}} \times v_{\text{water}}^2 \tag{4.12}$$

$$\lambda = 0.0317 \times \left(\frac{4 \times Q}{\pi \times d_{\text{pipe}}^2}\right)^{-0.15} \times (d_{\text{pipe, discharge}})^{-0.25} \tag{4.13}$$

$$R_{\text{additional}} = \xi_{\text{additional}} \times 0.5 \times \rho_{\text{water}} \times v_{\text{water}}^2 \tag{4.14}$$

$$R_{\text{static}} = (\mathsf{Z}_{\text{dredging}} + h_{\text{pump}}) \times g \times \rho_{\text{water}} \tag{4.15}$$

$$R_{\text{vacuum}} = (-g + \xi_{\text{water}} \times 0.5 \times v_{\text{water}}^2) \times \rho_{\text{water}} \tag{4.16}$$

$\lambda =$ Darcy-Weisbach friction factor $[-]$
$\xi_{\text{additional}} =$ Resistance factor for bends, valves, and nozzles $[-]$
$\xi_{\text{water}} =$ Resistance factor for water $[-]$

The pump-resistance curve of one WID's jet pump is given in Figure 4.6, and the parameters used are given in Table 4.3. The results were obtained with the jet pump working at 575 RPM on a dredging depth of 7 meters. The static head is determined by the dredging depth, the additional friction is mainly caused by the bends and nozzles in the jet system. This resulted in a working point of 1.52 m^3/s and

186.2.2 kPa. The power requirement according to Equation 4.7 equals 333.02 kW. The contribution of each resistance term to the resistance curve is seen in Figure 4.7.

Table 4.3: Example values

Parameter	Value	Unit
ρ_{water}	1025	kg/m^3
g	9.81	m/s^2
h_{pump}	0.5	m
$d_{\text{pipe, suction}}$	0.8	m
$d_{\text{pipe, discharge}}$	0.78	m
L_{pipe}	40	m
z_{dredging}	7	m
$\xi_{\text{additional}}$	22	–
RPM_{nom}	560	–

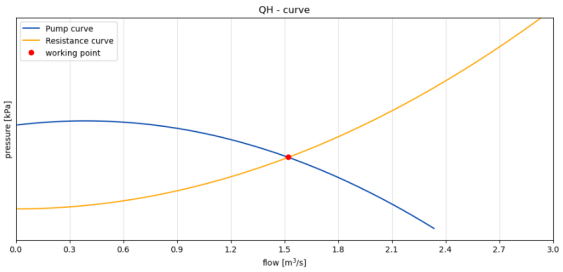

Figure 4.6: Pressure flow diagram **(Note: axis removed for confidentiality)**

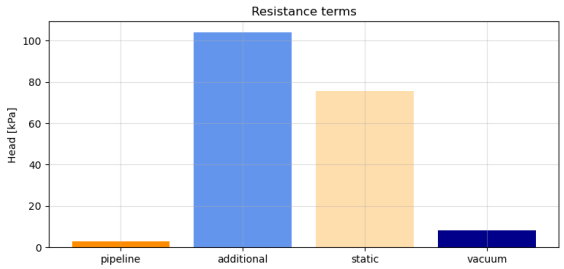

Figure 4.7: Resistance terms for Q = 1.52 m^3/s

4.3. Onboard module

The bow thruster on a WID ensures high maneuverability during low sailing velocities. The bow thruster is mainly used during the (un)mooring and the production phase when the velocity is low but high precision is needed. During the production phase, the WID sails back and forth in lines. After a line is completed, the vessel moves perpendicular to the line with the bow thruster and provides additional maneuverability during dredging and the use of DP.

Figure 4.8: Bow thrusters of the Rhone

The required power of the bow thruster is calculated by multiplying a factor with the installed bow thruster power. The scaling factor allows to calculate the energy by multiplying the thruster power P_{thruster} with the operation time to simplify calculations.

$$P_{\text{thruster}} = \alpha_{\text{thruster}} \times P_{\text{thruster installed}} \tag{4.17}$$

$$E_{\text{thruster}} = P_{\text{thruster}} \times t_{\text{operation}} \tag{4.18}$$

Where:

$\alpha_{\text{thruster}} =$ Scaling factor for bow thruster $[-]$
$P_{\text{thruster}} =$ Bow thruster power $[W]$
$E_{\text{thruster}} =$ Bow thruster energy use $[J]$
$t_{\text{operation}} =$ Time of operation $[s]$

During a WID's operation, more power consumers are active. These are grouped, as they will be modeled as constant values over time. The most important consumers are described in this section.

The onboard winches are responsible for two tasks during the dredging phase. The winches control the lowering and lifting of the jet beam at the start and the end of the operation, as well as regulating the height of the jet beam throughout the operation. As the vessel is subjected to vertical movement due to waves, the jet beam will also experience an unwanted corresponding vertical displacement.

The onboard electrical components are considered too. These include essential instruments like radar and sonar, but also onboard household appliances. These components are grouped, and a constant value is taken for the power requirement. According to Van Koningsveld et al. (2021), an onboard power requirement of 5% of the total installed power can be taken for Inland Waterway Transport (IWT) vessels.

$$P_{\text{onboard}} = \alpha_{\text{onboard}} \times P_{\text{installed}} \tag{4.19}$$

$$E_{\text{onboard}} = \int P_{\text{onboard}} \times dt \tag{4.20}$$

Where:

$P_{\text{onboard}} =$ Onboard electronics power $[W]$
$\alpha_{\text{onboard}} =$ Onboard electronics constant $[-]$
$P_{\text{installed}} =$ Total power installed $[W]$
$E_{\text{onboard}} =$ Onboard electronics energy use $[J]$

4.4. Simulation modules overview

This section gave an answer to Research Question 3:

How can currently unavailable estimating modules for a WID be developed to enable comparison of WID-based work methods with conventional dredging work methods?

To compare the emissions of a WID with other dredging methods, three modules are utilized to estimate the power requirement of a WID. The modules were developed or adapted from previous research, as they were unavailable for the implementation of WID's maintenance works. The propeller module calculates the propulsion power using the method proposed by Holtrop and Mennen, where the total resistance of the vessel is calculated to determine the required propulsion power. The power requirement of the jet pumps is calculated by the pump module, using affinity laws to calculate the output of the jet pumps when the pump speed is changed. The final module covers the bow thruster and board net appliances, where both power consumers are simulated using a scaling factor.

Different dredging work methods can now be compared using these modules, as they have been adapted to WID. The results of the modules facilitate the comparisons because they employ the same methodology or technique, regardless of the dredging equipment they are applied to. Furthermore, the modules can be incorporated into the OpenCLSim tool with the energy plugin explained in Chapter 3. The results of the implementation of the modules with the energy plugin are given in Chapter 5.

5 Simulations

In this chapter, the approach and the results of the case study comparison are given. The comparison of a WID with a TSHD is done by conducting a case study, which is first simulated with a WID to analyze the results. The case study is repeated with identical parameters for a TSHD, allowing to compare both results of the simulations.

5.1. Case study

The Ramsgate project spanned three weeks, commencing on 16th June 2024 and concluding on 3th July 2024. Ramsgate is a coastal city in the South-East United Kingdom with 40,000 inhabitants, shown in Figure 5.1. The port of Ramsgate consists of two parts, a marina for recreational vessels and a port area to accommodate RoRo ferries. The port area and marine area are given in Figure 5.2.

Figure 5.1: Satellite image of the UK with Ramsgate highlighted by a red dot (Google Earth, 2024)

Figure 5.2: Zoomed satellite image of Ramsgate, with the port area (blue) and marine area (orange) shown. (Google Earth, 2024)

The port of Ramsgate has an entrance channel to accommodate RoRo ferries, which is kept at a minimum of 7.5 meters. The port area is kept at a minimum of 7 meters. The tidal range is 4.6 meters, with Mean High Water Springs (MHWS) at 5.2 and Mean Low Water Springs (MLWS) at 0.6 meter. The working area of the project, with the entrance channel to the ferry and to the marine area, is illustrated in Figure 5.3.

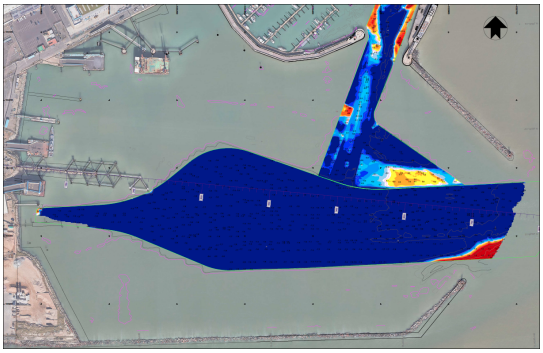

Figure 5.3: The dredging area of the Ramsgate project

Figure 5.4: Newest generation WID: MAAS

The parameters used in this case study are given in Table 5.1 and Table 5.2. The vessel parameters and the parameters SFC and TTW are extracted from the vessel database of Van Oord. The SoD, jet pump RPM, and production parameters are extracted from the vessel logs. The used vessel for this case study is the WID MAAS, the newest generation of WIDs of Van Oord, shown in figure 5.4. The vessel is equipped with a hybrid management system, allowing it to store rest heat in the batteries for later use. In addition, the vessel is also equipped with heave compensation for the jet system and dynamic positioning for positioning during dredging operations.

Table 5.1: Site parameters Ramsgate **(Note: dummy values are employed for confidentiality)**

Site input	Value	Unit
Soil type	Sandy-silt	$-$
Particle size	65	μm
Situ density	1,500	kg/m^3
Particle density	2,600	kg/m^3
Water density	1,025	kg/m^3
Mean water depth	7	m
Tidal amplitude	2.3	m
Dredging area	80,000	m^2
Mean distance to HEE	400	m
Volume to be dredged	270,000	m^3
Operational factor	0.75	$[-]$

Table 5.2: Vessel parameters Ramsgate **(Note: dummy values are employed for confidentiality)**

Vessel input	Value	Unit
Dredging velocity	0.514	m/s
Port sailing velocity	2	m/s
Diameter jet pipe	0.6	m
Length jet pipe	30	m
Length	25	m
Draught	1.50	m
Width	8.40	m
Jet beam width	9	m
SoD	0.5	m
Jet pump	600	RPM
α_{SFC}	41.2	g/MJ
α_{TTW}	3.2024	$-$
$\zeta_{\text{additional}}$	10	[$-$]

The site and vessel parameters allow to define the sites, vessel, and activities in OpenCLSim. Table 5.3 portrays the plugins that are implemented for each activity and its function. Table 5.4 shows the mixins that are used to define each object in OpenCLSim, allowing to simulate a WID, dredging site, and port site. Once all parameters, activities, sites, and vessels are defined, a while statement is formulated to ensure all sediment is dredged at the designated site for the simulation to be finished.

Table 5.3: Overview of the activities with corresponding plugin and input parameters

Activity	Function	Plugin	Input
Preparing	Simulates the period outside the tidal window	Energy plugin Tidal plugin	Time
Dredging trip	Simulates the trip from the berth to the dredging site	Energy plugin	Time Distance
Dredging	Simulates the dredging period	Energy plugin	Volume Velocity
Port trip	Simulates the trip from the dredging site to the berth	Energy plugin	Time Distance

Table 5.4: Site and vessel definition

Object	Identifiable	Log	Locatable	HasContainer	HasResource	Movable	WIDprocessor
WID	x	x	x	x	x	x	x
Dredging site	x	x	x	x	x		
Port site	x	x	x				

During the dredging activity, the vessel exhibits a back-and-forth motion in reality, which is not simulated in OpenCLSim. As OpenCLSim is a discrete event simulation package, the passage of time is only relevant concerning the occurrence of events, rather than being a continuous variable. This allows the exclusion of schematizing specific movements within an activity. The input parameters are the velocity and volume of dredged material, determined by the production rate and the duration of the activity. The inputs for the sailing trips are time and velocity, for the preparation activity the only input is time.

During the case study, a tidal window was utilized, during which the vessel dredges for six hours. The production rate is estimated using the factor-based method. As a tidal window is employed during this project, it is assumed that the out-of-service hours have already been accounted for, including periods of downtime resulting for maintenance and bunking. To account for any operational delays, such as turning or waiting for passing traffic, a factor ($f_{\text{operational}}$) is employed. This factor is derived from in-house experience at Van Oord in WID's operations and is assumed to be constant for various maintenance dredging operations. The operational factor is used in Equation 5.1 to calculate the volume of dredged material per tidal window (V_{dredging}), by multiplying the total duration of the dredging window ($T_{\text{window}} \approx 6$ hr) with the production rate ($Q_{\text{production}}$). All parameters used in the simulation are now defined, allowing to conduct the case study.

$$V_{\text{dredging}} = Q_{\text{production}} \times (T_{\text{window}} \times f_{\text{operational}}) \tag{5.1}$$

5.2. WID

5.2.1. Project results

The conducted case study resulted in the project results. The simulated power distribution is visualized in Figure 5.5, the energy consumption per activity is given in Figure 5.6. It is evident that the jet pumps are the primary source of energy consumption during the operation of a WID.

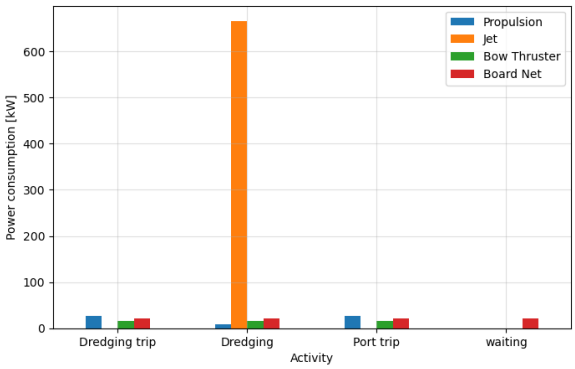

Figure 5.5: Power required per activity

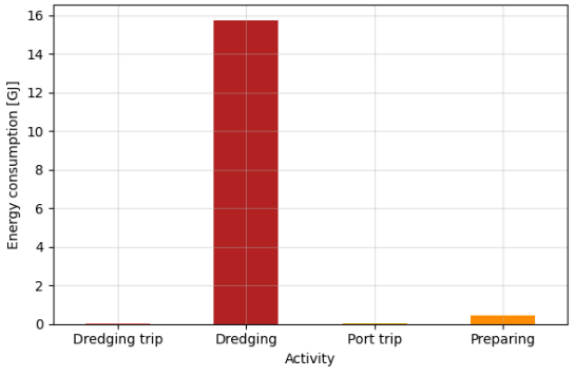

Figure 5.6: Energy required per activity

The values of the simulated power requirement are presented in Table 5.5. The jet pumps significantly consume the most power during the dredging activity. This is also the longest activity, resulting in the highest energy consumption, as shown in Table 5.6 where the amount of energy consumption, fuel consumption, and emissions are given for each activity.

Table 5.5: Project results: simulated power requirement per activity **(Note: dummy values are employed for confidentiality)**

Parameter	Dredging trip	Dredging	Port trip	Waiting	Unit
Propulsion	26.396	8.350	26.396	0.00	kW
Jet pumps	0.00	665.746	0.00	0.00	kW
Bow thruster	16.020	16.020	16.020	0.00	kW
Board net	20.880	20.880	20.880	20.880	kW

Table 5.6: Project results: calculated energy, fuel and emissions per activity **(Note: dummy values are employed for confidentiality)**

Parameter	Dredging trip	Dredging	Port trip	Waiting	Unit
Duration	0.056	6.154	0.056	6.152	hr
Energy	0.013	15.751	0.0123	0.462	GJ
Fuel	0.311	382.307	0.311	11.225	kg
Emissions	0.996	1223.916	0.996	35.934	kg

The energy, fuel and emissions results for the whole project are shown in Table 5.7, where the energy, fuel and emissions per cubic meter dredged are calculated by Equation 5.2:

$$\text{Energy per cubic meter dredged, total project} = \frac{E_{\text{total project}}}{V_{\text{total project}}} \tag{5.2}$$

The total energy of the project ($E_{\text{total project}}$) is 535.48 GJ and the total volume of the project to be dredged ($V_{\text{total project}}$). This results in the energy footprint per cubic meter dredged material, which serves as a KPI for comparison with other dredging techniques.

Table 5.7: Project results: Energy, fuel and emissions of total project and per cubic meter dredged

	Project totals		**Per cubic meter dredged**	
Parameter	**Value**	**Unit**	**Value**	**Unit**
Energy	535.48	GJ	3.966	MJ/m^3
Fuel	12,997.03	kg	0.096	kg/m^3
Emissions	41,608.68	kg	0.308	kg/m^3

The energy, fuel, and emissions results for the dredging activity only are repeated in Table 5.8, and the energy, fuel, and emissions per cubic meter dredged are calculated using Equation 5.3:

$$\text{Energy per cubic meter dredged, dredging activity} = \frac{E_{\text{dredging activity}}}{V_{\text{dredging activity}}} \tag{5.3}$$

The energy consumption of the dredging activity ($E_{\text{dredging activity}}$) is 15.751 GJ, and the volume of dredged material during the activity ($V_{\text{dredging activity}}$) is 4,184.9 m^3. In this analysis, the energy per cubic meter is based entirely on the dredging activity, rather than including the sailing and preparing activities.

Table 5.8: Dredging activity results: Energy, fuel and emissions of dredging activity and per cubic meter dredged **(Note: dummy values are employed for confidentiality)**

	Dredging activity		**Per cubic meter dredged**	
Parameter	**Value**	**Unit**	**Value**	**Unit**
Energy	15.751	GJ	3.764	MJ/m^3
Fuel	382.307	kg	0.091	kg/m^3
Emissions	1,223.916	kg	0.029	kg/m^3

An overview of the simulated and measured project results is provided in Table 5.9. There were more operational hours simulated than measured, while fewer trips were performed, meaning that each trip had fewer operational hours measured than simulated. The production rate was underestimated slightly, and the operational factor was assumed correctly.

Table 5.9: Overview simulated and measured project results **(Note: dummy values are employed for confidentiality)**

Parameter	Simulated	Measured	Unit
Project duration	403.7	417.5	hr
Operational hours	201.9	187.4	hr
Trips	33	34	$[-]$
Production rate	850.1	900.5	m^3/hr
Operational / total hours	80	80.70	$\%$

5.2.2. Modules results

The outcomes of the propeller module, the propulsion power for each activity, are verified by dividing the sailing activities into three segments. The segments are selected based on different characteristics, detailed in Table 5.10. Segment three is used for verification of the propeller module and is not incorporated in the simulation of the case study, as it includes the part where the vessel sails to the project area in Ramsgate. The results of segment three are removed due to confidentiality. The propulsion power and velocity are measured for each segment, after which the velocity is used as input for the propeller module. The output of the propeller module is compared to the measured propulsion power.

Table 5.10: Sailing segments with corresponding characteristics

Segment:	1	2	3
Description	Dredging	Port - dredging	Rotterdam - Ramsgate
Shallow water	Yes	Yes	No
Submerged jet beam	Yes	No	No

In the first segment, the vessel dredges in the sheltered port area with shallow water with a submerged jet system. Figure 5.7a shows the velocity profile of the project, including the dredging mode. The state signal indicates which dredging mode is active, allowing to filter the signal while dredging. A total of 34 dredging trips were identified, with Figure 5.7b illustrating the velocity profile with the status signal for a single dredging trip. It is seen how the velocity signal spikes before dredging, where the vessel sails from its berth to the dredging site, indicating the importance of filtering the signals.

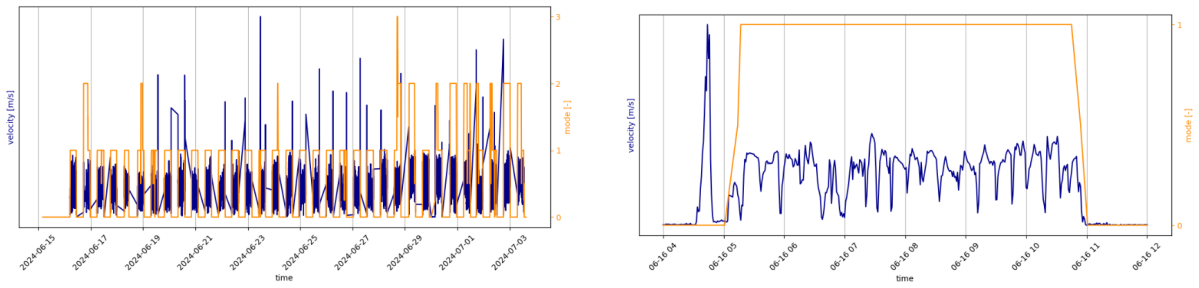

(a) Velocity profile and dredging mode of the full project **(Note: axis removed for confidentiality)**

(b) Velocity profile and dredging mode of a single dredging trip **(Note: axis removed for confidentiality)**

Figure 5.7: Velocity profile and dredging mode; blue plot represents the velocity, orange plot indicates the dredging state signal

The velocity profile of Figure 5.7b shows significant fluctuations. This is explained as the WID sails back and forth in a zig-zag motion, slowing down each time to reverse its velocity. Figure 5.8 shows the boxplot of the propulsion power per velocity interval. The interval with the lowest velocity range displays the highest number of outliers, indicating a large spread in the data. Additionally, the interquartile range (IQR, representing the central 50% of the data) of propulsion power of each interval is spread too. The mean velocity while dredging is $v_{\text{mean}} = 0.46$ m/s. The mean measured power requirement is 63.8 kW, as shown in Table 5.11.

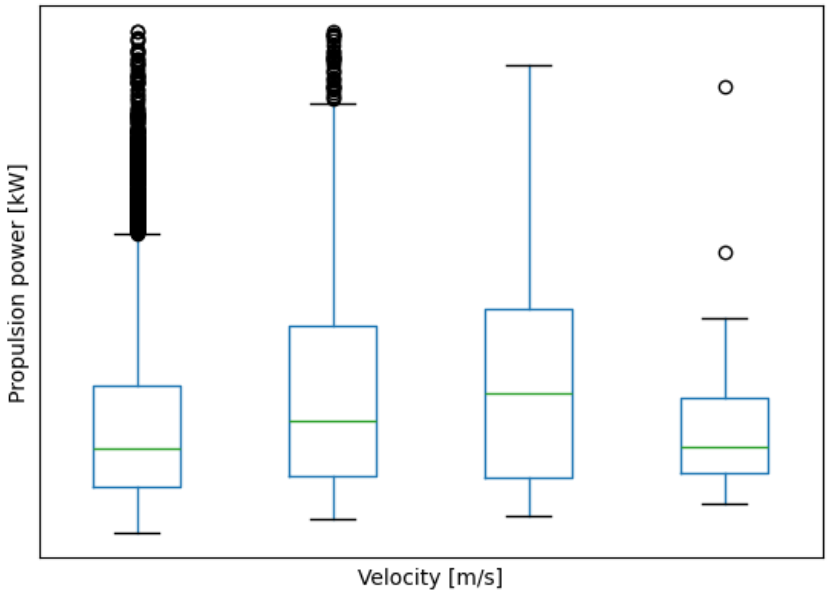

Figure 5.8: Boxplot of dredging data by velocity interval: Medians (green lines), IQR (blue boxes), and outliers (black circles) **(Note: axis removed for confidentiality)**

Table 5.11: Propulsion power, sailing while dredging

Parameter	Value	Unit
Average velocity measured	0.48	m/s
Average power measured	63.78	kW
Average power calculated	8.35	kW

The second segment was chosen to represent the periods the vessel is sailing in shallow water with an emerged jet system. To validate this section, the data is filtered first, based on when the vessel is moving without dredging. Each trip was filtered by using the dredging state signal. These intervals are summarized in Table 5.12. Figure 5.9 shows the Ramsgate port area with the berthing location, indicated with the red circle.

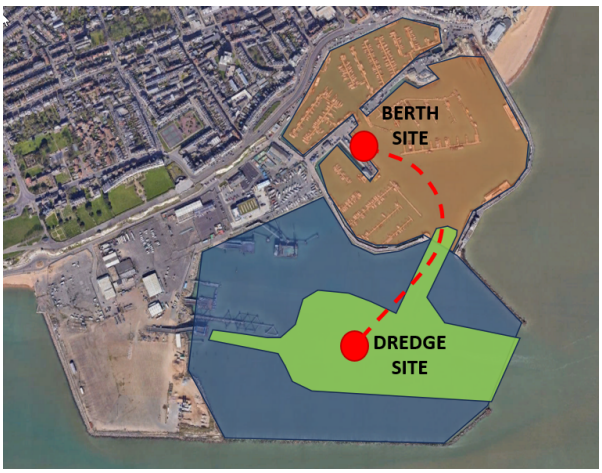

Figure 5.9: Ramsgate area with dredge and berth sites and the route shown with dashed red line

The mean velocity is used as input to estimate the propulsion power. The duration is used to calculate the energy consumption. The duration and distance are used for simulating the segment in OpenCLSim.

The calculated value for the propulsion power corresponding to the mean measured velocity is P_{prop} = 10.93 kW

Table 5.12: Berth-dredging trips summarized

Parameter	Mean value	Unit
velocity	0.57	m/s
measured propulsion power	42.28	kW
calculated propulsion power	10.93	kW
duration	557.57	s
distance	405.87	m

The outcomes of the pump module are separately described in this section, where the power output of the jet pumps and the corresponding state signal are given in Figure 5.10. The state signal indicates whether dredging is occurring, used to filter the data. Furthermore, the water level is plotted in the same graph with the used power requirement, allowing to examine the dredging windows of this operation. It can be seen in Figure 5.11 that the operation starts circa 2 hours before the outgoing tide starts.

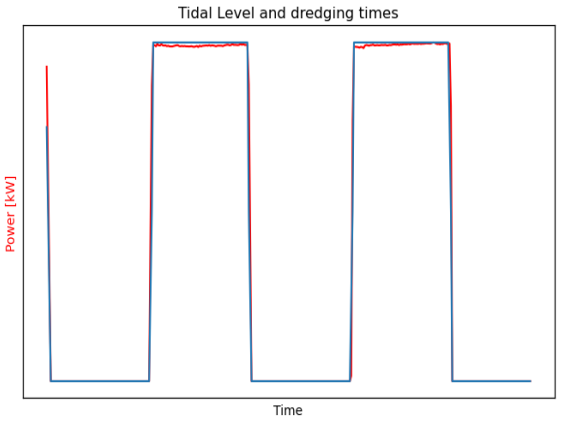

Figure 5.10: State signal and jet pump power **(Note: axis removed for confidentiality)**

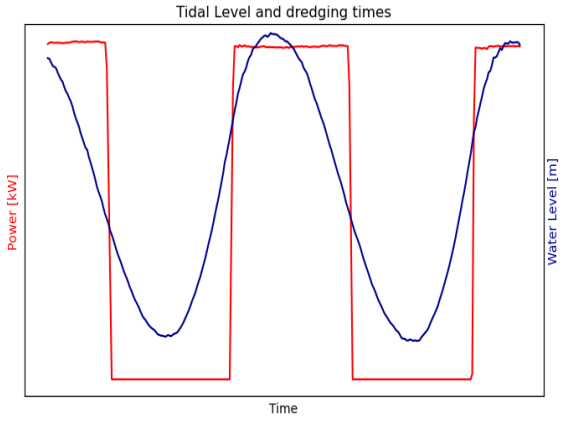

Figure 5.11: Dredging windows visualized **(Note: axis removed for confidentiality)**

The power, pressure, and flow are calculated with the average measured RPM as input for the pump module. The results of the pump module are presented in Table 5.13, where it can be observed that the pump module underestimates the power, while the pressure and flow are calculated correctly.

Table 5.13: Mean values one jet pump

Parameter	Value (measured)	Value (calculated)	Unit	Error
RPM	575	-	–	-
Power	693.24	615.04	kW	11.28 %
Pressure	186.25	178.04	kPa	4.41 %
Flow	2.952	2.940	m^3/s	0.41 %

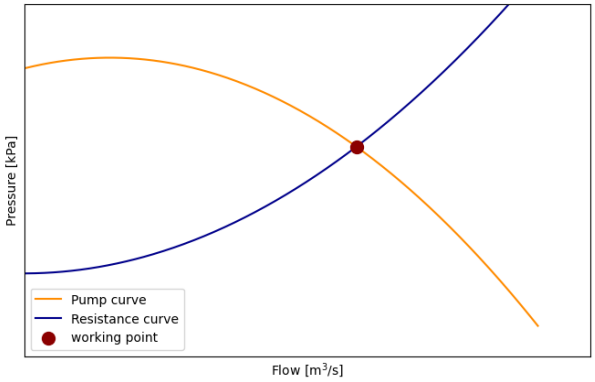

Figure 5.12: Pump and resistance curve for one pump with the working point given with the red dot **(Note: axis removed for confidentiality)**

The bow thrusters and board net power consumers are components that are calculated in the onboard module with a scaling factor α_{thruster} and $\alpha_{\text{board net}}$, respectively. It should be noted that the values are not a result of a simulation, but have been extracted from the vessel logs. This has been done under the assumption that the values remain constant with different projects. The scaling factors are used for the onboard module components to simplify a complex process, and to allow for fine-tuning the onboard module.

Figure 5.13 illustrates the signal of the bow thruster, indicating that the maximum available bow thruster power and the propulsion power are always in use during sailing. The resulting Equation 5.4 yielded in a scaling factor α_{thruster} = 0.06.

$$\alpha_{\text{thruster}} = \frac{P_{\text{thruster, mean}}}{P_{\text{thruster, max installed}}} \tag{5.4}$$

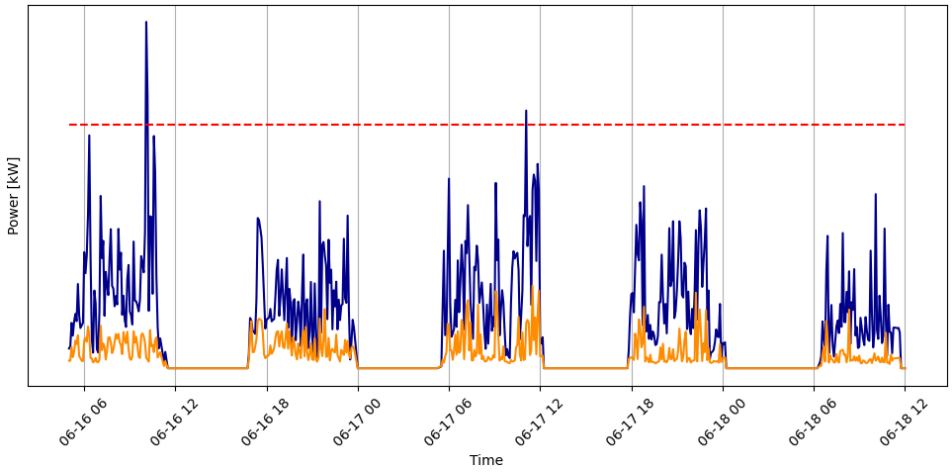

Figure 5.13: Propulsion power, measured & max installed bow thruster power **(Note: axis removed for confidentiality)**

The auxiliary engine of a WID is responsible for supplying the necessary power for the operation of the vessel's onboard appliances when the vessel is moored at its berthing location. If the vessel is engaged in sailing or dredging activities, the power requirement of the onboard appliances is provided by the main generators, and calculated with Equation 4.19. Figure 5.14 illustrates the power requirement of the auxiliary engine and propulsion, indicating that the auxiliary engine is only used when the vessel is docked. The calculations yielded an $\alpha_{\text{board net}}$ value of 0.24, which would result in a simulating value $P_{\text{board net}}$ = 21.27 kW.

$$\alpha_{\text{board net}} = \frac{P_{\text{board net, mean}}}{P_{\text{board net, max installed}}} \tag{5.5}$$

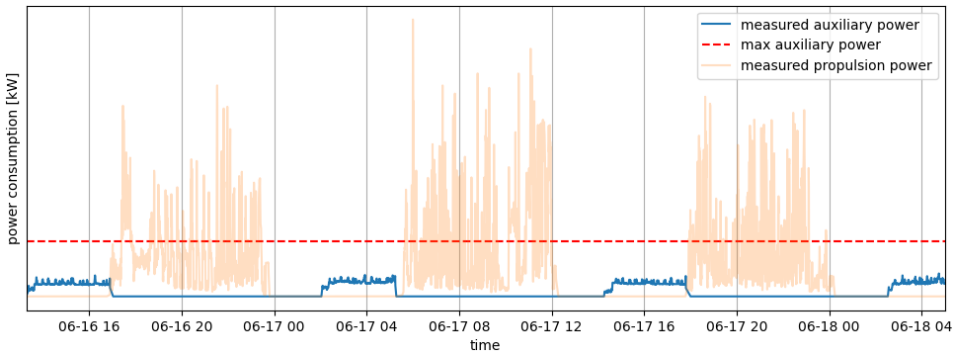

Figure 5.14: Propulsion power and measured auxiliary power **(Note: axis removed for confidentiality)**

5.2.3. Output analysis

This subsection analyses the findings of the individual modules in the conducted case study, which are summarized in table 5.14 with the corresponding relative error.

Table 5.14: Overview of the individual modules with estimated and measured values with the relative error

Module	Activity	Estimated [kW]	Measured [kW]	Relative error [%]
Propeller	Sailing	10.93	42.28	74.15
	Dredging	8.35	63.78	86.91
Pump	Dredging	615.04	693.24	11.28

The propeller module was used for two activities in the model, where the module significantly underestimated the propeller power in both activities. The sailing activity was underestimated by 75%, and the dredging activity with 87%.

During the dredging activity, more actuators than the velocity influence the required propulsion power. Figure 5.15 shows the data points for a single dredging trip, where k-clustering is applied to the data. K-clustering results in two clusters, where each cluster represents a set of data points that are similar in characteristics, allowing for identifying patterns. Table 5.15 portraits a summary of the clusters, where both clusters have the same range of velocities, while cluster 0 has a significant lower propulsion power average than cluster 1.

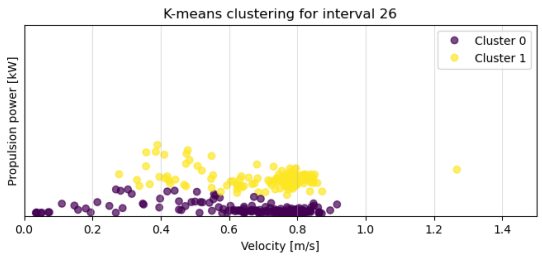

Figure 5.15: K-clustering of a dredging trip data points

Table 5.15: Summary of k-clustering

Cluster	Propulsion power [kW]	Velocity [m/s]
0	21.70	0.66
1	115.79	0.72

The clusters are visualized in Figure 5.16, illustrating the variations between individual runs, during which the vessel operates in a single direction. This indicates that the vessel requires alternating propulsion power due to the tidal current as it sails with the direction of the current on one run, and

against the current on the following run. Figure 5.17 portraits the tidal currents in the port of Ramsgate, which are not extracted from the vessel logs but from the Ramsgate Port Authority. The addition of an average tidal velocity of 0.7 m/s to the vessels average velocity will result in an estimated power requirement of 60.15 kW, which is still a relative error of 48% for a single run. It is believed that the currents influence the magnitude of the propulsion power errors, but are not the sole explanation as the module also underestimates during sailing with an emerged jetbeam.

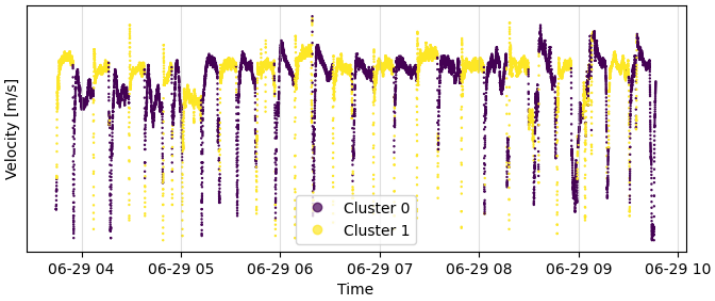

Figure 5.16: K-clustering visualized over the velocity signal of a single dredging trip

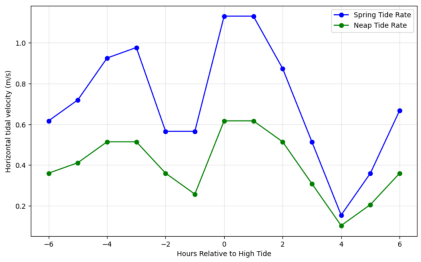

Figure 5.17: Tidal currents in Ramsgate (Ramsgate Port Authority, 2024)

Additional causes for the significant underestimation during the dredging activity can be partially attributed to the vessel exhibiting a zigzag movement, where the velocity direction is reversed each time. This results in peaks in the required power as the vessel needs to (de)accelerate each time. Furthermore, as shown in Figure 5.18, the vessel sails in both directions causing the jet beam to be pushed through the fluidized sediment layer created at the previous run. Additionally, the jet beam has a SoD of 0.4 meters, which could cause additional resistance effects due to the restriction of flow around the jet beam and the bed.

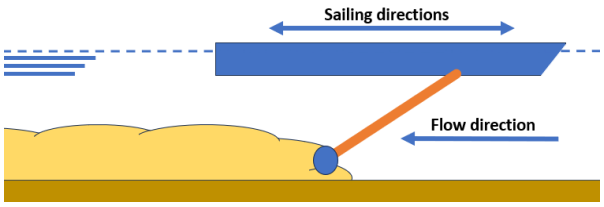

Figure 5.18: Schematized WID: sailing through fluidized sediment layer

The propulsion power during the sailing phase was significantly underestimated as well. However, it should be noted that the average sailing trip is 400 meters in length, which contributes to the difficulty of accurately estimating the propulsion power. This is because the vessel is (de)accelerating for the majority of the time, and thus it does not sail with a constant velocity.

The pump module consumes a significant proportion of the used power on board the vessel and in addition, the jet pumps are almost 50% of the time operational, making it the most important module for correctly estimating the energy consumption. The underestimation of 10% of the pump module is attributed to the heavy wear and tear of impellers, leading to an increased power demand.

The vessel logs indicate that a tidal window was utilized, shifted approximately 1.5 hours earlier than the onset of the outgoing tide. This adjustment ensures that sediment is already fluidized by the start of the outgoing tide. Similarly, the reasoning applies to the end of the tidal window, where it is recommended to cease dredging operations to prevent sediment from remaining fluidized without sufficient time for transport out of the system by the tidal current.

The vessel logs for the auxiliary engine, which provides the power for the board net when the vessel is moored, indicate a period between dredging operations and the deployment of the auxiliary engine. This interval, during which no power is generated by the engines, is the result of the stored energy of the engines' rest heat used to charge the batteries, which are then used if the vessel is moored. This is not directly incorporated in the simulation; however, by utilizing a scaling factor for the board net, it is accounted for as the mean value of the power output over the whole operation is taken.
The scaling factor for both the bow thrusters and the board net can be vessel specific, depending on the vessel characteristics and the operational profile.

5.2.4. Output sensitivity

As seen in the output analysis, the propeller and pump modules underestimate the power requirement, thereby affecting the total energy consumption. To evaluate the impact of the modules on the project outcomes, the model is executed with the measured power requirement, shown in Table 5.16, which resulted in an energy consumption of 560.60 GJ. Despite the propeller module underestimating the power requirement by 75%, the total energy is increased by only 5%. This is caused by the vessel waiting in the port for the right tidal conditions when no propulsion or jet pump power is required limiting the influence of the simulating errors. Additionally, the energy distribution in Figure 5.6 shows that duration causes the jet pump to dominate the energy footprint, with little influence of the propeller module. It should be noted that the calculation of the total project energy is based on the adjustments of only the power requirement for the simulation, where the project duration, operational hours, and production rate are maintained at the levels estimated in the simulated case study.

Table 5.16: Simulation result with measured power requirement values

Values	Simulated	Measured	Unit	Error
Propeller module	10.93	42.28	kW	74.15 %
	8.35	63.78	kW	86.91 %
Pump module	615.04	693.24	kW	11.28 %
Total project energy	535.48	560.60	GJ	4.69 %

5.3. TSHD

This section presents the results of the simulation conducted with a TSHD first, to compare with the results of the simulation conducted with the WID after. However, before a TSHD can be applied to the Ramsgate project, it is necessary to revise the production rate estimation.

A schematic illustration of a TSHD's draghead is provided in Figure 5.19. The production rate is calculated by Equation 5.6, in which the cutting depth is governed by two mechanisms. The water jets are employed to cut through and break up the soil, contributing to an increased cutting depth beside the teeth of the draghead.

$$Q_{\text{draghead}} = v_{\text{trailing}} * W_{\text{draghead}} * (h_{\text{cutting, teeth}} + h_{\text{cutting, jets}}) \tag{5.6}$$

Where:

$Q_{\text{draghead}} =$ Draghead production $[m^3/s]$
$v_{\text{trailing}} =$ Trailing velocity $[m/s]$
$W_{\text{draghead}} =$ Draghead width $[m]$
$h_{\text{cutting}} =$ Cutting depth $[m]$

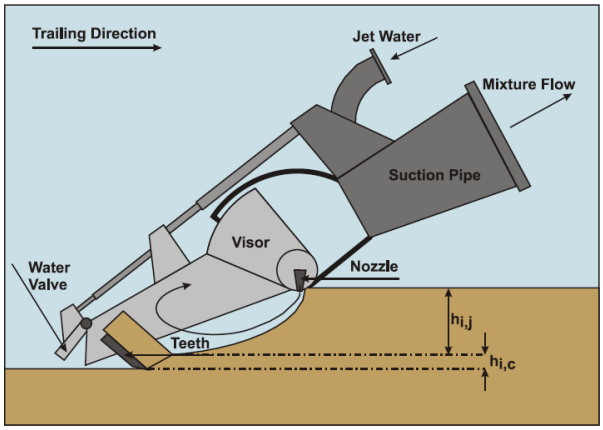

Figure 5.19: Schematized draghead of a TSHD (Miedema, 2019)

The soil in the port of Ramsgate is composed of fine sediments, which can be effectively removed without the disintegration of the soil by the water jets. The low weight and shear strength of fine sediments often necessitate the use of only the teeth to reach the desired cutting depth. In addition, the high-pressure water jets of a TSHD will agitate and disperse the fine sediments, which will result in a lower production rate. For these reasons, it has been decided that the TSHD will not utilize the water jets during the dredging process.

The discharge location for the TSHD is selected according to the soil investigations conducted at the port of Ramsgate, which is situated at North Goodwin, located to the south of Ramsgate at a distance of 9.0 nautical miles. For this project with a TSHD, there is no tidal window in place.

The volume of material dredged for a TSHD is dependent on the overflow of the hopper. As a mixture of water and sediment is placed in the hopper it is efficient for the production rate to overflow the hopper, where the water flows overboard while the sediment remains. However, in this case study, overflow is not allowed. This is set by the Port of Ramsgate Authorities, as the fine sediment can disperse through the water column and cause high levels of turbidity during overflowing. This results in a hopper that is partially filled with sediment and partially filled with water, where the ratio between the two is dependent on the porosity and ambient water drawn into the hopper.

5.3.1. Project results

The vessel and soil parameters used for the TSHD are given in Table 5.17 and 5.18. The selected vessel is a jumbo TSHD of the Van Oord fleet, where dummy parameters are used for confidentiality.

Table 5.17: TSHD vessel parameters **(Note: dummy values used for confidentiality)**

Parameter	Value	Unit
Sailing velocity	15.5	kn
Dredging velocity	3.7	kn
Length	200	m
Draught empty	8.5	m
Draught full	13.55	m
Width	32	m
Capacity	39,467	m^3

Table 5.18: HAM 318 soil parameters **(Note: dummy values used for confidentiality)**

Parameter	Value	Unit
Initial porosity soil	0.44	–
Porosity at cutting	0.50	–
Dilatancy	2.5E-5	–
Initial permeability	1.0E-8	–
Permeability at cutting	5.0E-6	–
Vlasbom coefficient	0.1	–
Soil compaction force	6	kg/cm^3
Situ density	1400	kg/m^3

The power distribution of the different components of a TSHD is given per activity in Figure 5.20, where the propulsion system requires significantly the most power.

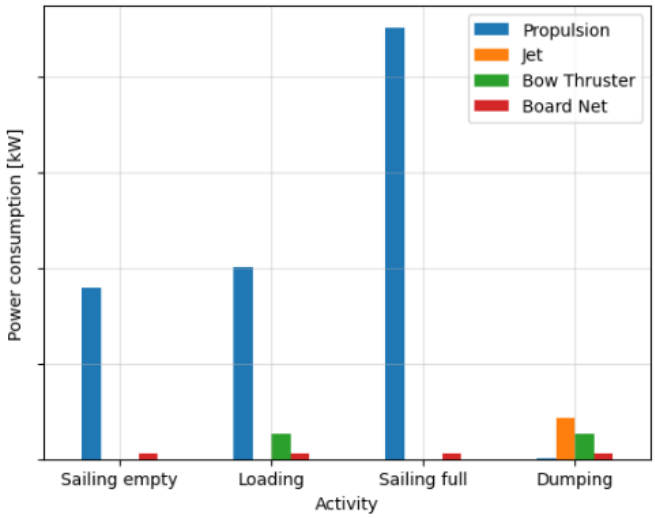

Figure 5.20: Power requirement of a TSHD's components per activity **(Note: axis removed for confidentiality)**

The power requirement over time is shown in Figure 5.21 for two days for the WID (left) and the TSHD (right), where only the common appliances are shown. The WID uses most of the power for the jet pumps and the propulsion power is low compared to the jet pumps. The TSHD consistently has a high propulsion power, with the jet pumps and bow thruster remaining at a relatively low constant level.

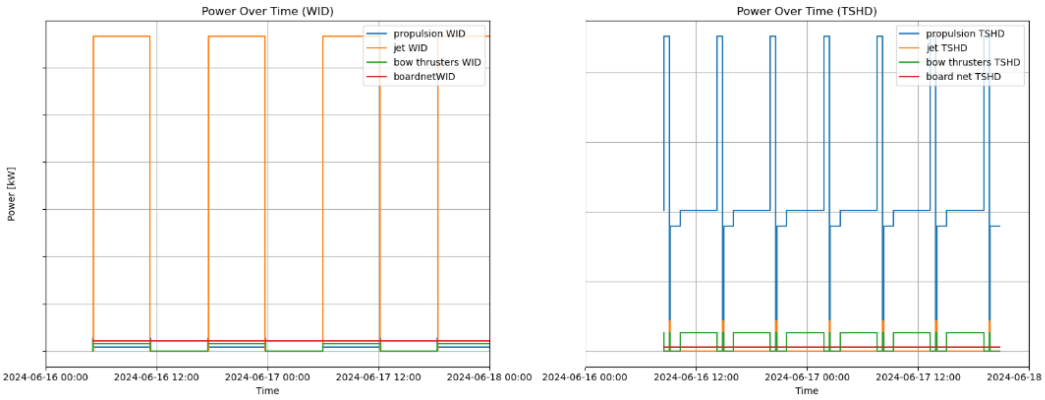

Figure 5.21: Power requirement of different components over time, for the WID (left) and the TSHD (right) **(Note: axis removed for confidentiality)**

The project totals are given in Table 5.19, where the energy, fuel, and emissions per cubic meter dredged for the total project, are calculated with Equation 5.2, utilizing the project volume ($V_{\text{total project}}$ = 135.001 m^3) and the total energy consumed ($E_{\text{total project}}$).

Table 5.19: Project results: Energy, fuel and emissions of total project and per cubic meter dredged for TSHD **(Note: dummy values are employed for confidentiality)**

	Project totals		Per cubic meter dredged	
Parameter	**Value**	**Unit**	**Value**	**Unit**
energy	2061.9	GJ	15.27	MJ/m^3
fuel	50,047.1	kg	0.37	kg/m^3
emissions	160,220.9	kg	1.187	kg/m^3

The production rate and duration of the project are presented in Table 5.20 along with the fuel consumption of the WID's and the TSHD's simulations, where the TSHD has a considerably lower project duration with a higher production rate, yet the WID consumes less fuel in total.

Table 5.20: Comparison production rate, duration, and fuel consumption of a WID and a TSHD **(Note: dummy values are employed for confidentiality)**

Parameter	**WID**	**TSHD**	**Unit**
Production rate	850.1	9844.2	m^3/hr
Project duration	403.7	36.33	hr
Total fuel	12,997.03	50,047.1	kg

5.3.2. Output analysis

It is noted that the used vessel, the HAM318, has a vessel length unpractical for the port of Ramsgate and a draught larger than the water depth, even if a tidal window would have been in place. In addition, an in-depth analysis of the power consumers and corresponding modules is lacking in this research, introducing uncertainty in the credibility of the results. For example, the calculations for the forces on the draghead were developed for coarse sediments and it was also mentioned that the propulsion power was underestimated by the model when the vessel sails with low velocity. The results were further obtained by assuming the soil parameters, which introduce uncertainty.

The results of the TSHD's simulation demonstrate that the propulsion power dominates the energy consumption. Especially during the sailing full trip, is the propulsion power significantly higher than the other power consumers, which consequently results in the distance between the dredge and dump site being an important factor in determining the total energy used. It is also noted that it is expected that the propulsion power increase and the production will decrease in real life. The same as with WID, the TSHD has to make a zig-zag motion during dredging to cover the whole area, which is done by turning and (de)accelerating. It is expected that this will increase the required propulsion power in real life. The turning and (de)accelerating is also expected to cause a decrease in production rate which causes an increased project duration.

5.4. Strategy comparison overview

This chapter presented a case study in the port of Ramsgate, which was used to conduct a simulation with a WID and a TSHD. The results were analyzed and compared. The approach used for the comparison of the results of the case-study simulations answered Research Question 4:

How can a WID-based work method for port maintenance be compared with conventional maintenance dredging work equipment?

The developed modules and the employed simulation tool facilitated the ability to analyze the power requirement over time and calculate the energy and fuel consumption. Utilizing the same simulation package, developing the modules necessary to quantify the power requirement, and using a case study to ensure that identical soil and site parameters are used, makes it possible to compare different port maintenance equipment. This is due to the obtained KPI's obtained from the simulation, the total project duration: the production rate and the specific fuel consumption facilitate straightforward comparisons to assess the production rate and the energy footprint.

6

Discussion

This chapter discusses the significance of this research in section 6.1. The main findings are discussed in section 6.2, where the outcome of this research is also compared to values found in the literature. The limitations of this research are given in section 6.3.

6.1. Research significance

The novelty of this research was the development of the WID activity, the tidal plugin, and a corresponding attribute, responsible for simulating a WID in a discrete event simulation package. The developed modules allow the production rate and power requirement to be estimated in the simulation. The production rate was estimated using empirical-based methods, which have not been done before. The significance of this research lies in the fact that this research advances the current state of the literature on maintenance dredging strategies with WID-based works. In addition, this research has extended the capabilities of the OpenCLSim package, thereby advancing the state of academic research. The developed model can be utilized by dredging contractors to gain insight into the power requirement of a WID throughout the project and to compare it with other dredging equipment. Additionally, this research contributes to the literature by being the first to compare a WID and a TSHD on energy consumption with a case study.

6.2. Research contribution

The main findings of the case study comparison are presented here. The conducted simulations demonstrated that a WID is not only more energy efficient for the total project duration but also in energy per cubic meter dredged.

For a WID, the fuel consumption per cubic meter dredged material was estimated, where two different methods were employed. The first method is by dividing the total fuel consumption by the total volume dredged of the project, the second method uses only the fuel consumed during the dredging activity and the volume of material dredged during the activity. The difference between the two values, 0.096 and 0.091 kg/m^3, shows that 95% of the fuel consumed is used for dredging.
This was also done for the TSHD, where the values were 0.37 and 0.265 kg/m^3, showing that 70% of the fuel consumed was used for dredging. Comparing the figures of a WID and a TSHD indicates that a WID uses a larger percentage of its energy for dredging than a TSHD, making it more efficient.

The fuel per cubic meter dredged is used for this comparison, allowing to compare the results of this study with the literature. In the literature, a broad comparison is made between a TSHD and a WID, and the results are given in Table 6.1. This research was done based on a maintenance dredging case study with a TSHD and a WID in the Port of Lisbon in 2014, where the fuel consumption was calculated using the total dredged volume and the total fuel consumption.

Table 6.1: Fuel consumption comparison for the case study in Lisbon (Vercruijsse et al., 2023)

Vessel	Capacity / Power	Dredged volume	Total fuel consumption	Fuel consumption
TSHD	2,500 m^3	200,000 m^3	98,500 L	0.5 L/m^3
WID	460 kW	800,000 m^3	38,500 L	0.05 L/m^3

The dredged volume and fuel consumption for the WID and the TSHD in the simulated case study are summarized in Table 6.2. A comparison of the fuel consumption data reveals that the fuel consumption of the WID in Lisbon is lower than the simulated fuel consumption of the Ramsgate project. However, the fuel consumption of the TSHD in Lisbon is higher than the fuel consumption of the simulated fuel consumption of the Ramsgate project. In the literature of Van Oord a general calculation has been done for the specific fuel consumption of a WID, 0.16 L/m^3, meaning that a conservative calculation has been done by Van Oord compared to this research.

Table 6.2: Fuel consumption comparison for the simulated case study [1]

Vessel	Capacity / Power	Dredged volume	Total fuel consumption	Fuel consumption
TSHD	39,467 m^3	135,001 m^3	58,879 L	0.435 L/m^3
WID	800 kW	135,001 m^3	15,290 L	0.113 L/m^3

It is important to consider the significant discrepancy in the maximum jet pump power, and thus fuel consumption, between the vessels in Lisbon and Ramsgate. Furthermore, the soil, vessel, and hydrodynamic parameters are unknown, thus the production rate is unknown. The total volume of dredged material was greater than in Ramsgate, which can lead to a more efficient and thus a high production rate. This resulted in an operation that is more fuel-efficient consumption per cubic meter dredged. The TSHD in Ramsgate has a lower fuel consumption than in Lisbon, which is caused as turning and maneuvering are not simulated and would result in a significantly higher fuel consumption than concluded.

6.3. Research limitations

The limitations of this study are presented in this section. The cause of the largest discrepancies between the simulated and measured values originates in the propulsion module, although it was shown that the pump module is the dominant factor for the total energy consumption.

The method proposed by Holtrop and Mennen has been developed for application to cargo vessels sailing in open sea, with a constant velocity. In this study, the method was applied to the WID, resulting in significantly underestimated values. The vessel criteria for which this method was developed have fundamental differences from a WID, listed in Table 6.3. The methodology was adopted to accommodate shallow water conditions and was used for simulating the propulsion power of a TSHD, which has comparable dimensions to those of a cargo vessel. A significant impact on the accuracy of the propeller module is caused by the sailing velocity. The method is based on the sailing velocities of cargo vessels, which range between 15 - 25 knots (Chakraborty, 2024). For low sailing velocities, the power estimation is very sensitive to velocity changes due to the exponential relationship between velocity and propulsion power.

[1] kg/m^3 has been converted to L/m^3, using ρ_{fuel} = 0.85 kg/L.

Table 6.3: Differences between cargo and WIDs

Criteria	Cargo vessel	WID
Design vessel	Efficient transportation of cargo	High maneuverability and stability
Shape	Long, narrow and deep draft	Short, wide and shallow draft
Environment	1) Deep sea water	1) Shallow port areas
	2) Long waves	2) Short waves
Sailing velocity	15 - 25 knots	1 knots
Velocity profile	Long durations & constant	Short durations & fluctuating

A dredging window was employed in this project, resulting in six-hour periods of dredging, twice a day. The dredging window was simulated using the tidal plugin, which demonstrated the expected functionality. It is important to note that the tidal plugin signal is based on solely the M2 constituent, which results in a perfect semi-diurnal (twice a day) tide as illustrated in Figure 6.1. In reality, the tidal signal is based on multiple constituents, resulting in the daily, monthly, and seasonal variation in low and high water levels, as shown in Figure 6.2. The difference in tidal water levels will result in an inaccurate estimation of the production rate. To avoid this limitation, daily tidal levels should be calculated and used for the production rate estimation.

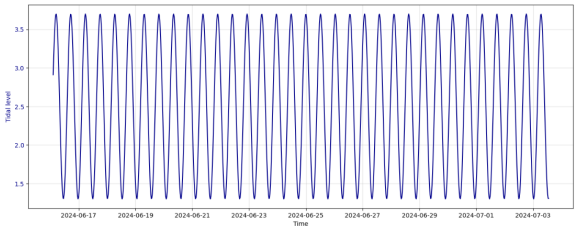

Figure 6.1: Simulated tidal signal

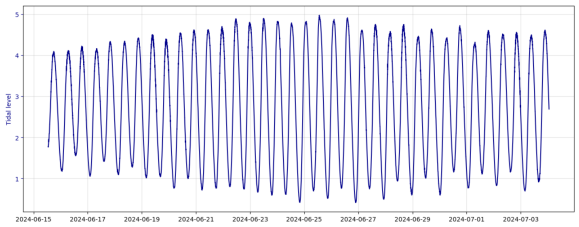

Figure 6.2: Measured tidal signal

The bow thrusters and the onboard appliances are represented as a constant over time in the simulation, which is not an accurate representation of reality because the bow thruster is only used in short bursts, either under the control of the captain during mooring or under control by the DP-DT system during dredging.

It was assumed that the production rate remains constant over time. In practice, the soil parameters are not constant with time, area, and depth. Loose and freshly deposited material is dredged first, and more compacted material is dredged later. This results in a decreasing production rate as the cohesion strength of the material increases. Additionally, the production rate of a WID is heavily dependent on its crew. The captain decides where and which dredging mode is used, depending on the objective, morphology, and soil parameters. Furthermore, an underestimation of the production rate may also be attributed to the soil input. It is noted that two investigations for the soil conditions are available, one conducted in 1995 and the other conducted as part of the in and out survey. The soil investigations yielded varying results, particularly with regard to the grain size and the total dredging volume.

It is important to acknowledge the limitations of the TSHD's applicability to shallow water as Ramsgate. It should be noted that this research was focused on specific vessels, namely the WID Maas and the TSHD HAM318. The method employed to estimate the production rate of a TSHD should only be applied to saturated sand and not the fine material present in Ramsgate. Furthermore, the efficiency ratio between a WID and a TSHD was calculated under specific assumptions, necessitating caution when interpreting the results.

To summarize, the following limitations to this research were acknowledged:

- The applicability of the method proposed by Holtrop and Mennen.
- A simplification of an accurate tidal signal.
- A simplification of the different dredging modes and corresponding production rates.
- The horizontal tidal currents are not taken into account.
- A constant production rate estimation is assumed.
- Variability in soil investigation results.
- The employed estimating method for the TSHD's production rate was not designed for fine material.
- The employed TSHD in this research is not able to physically dredge in Ramsgate due to its dimensions.

It should be noted that not all limitations impact the precision of the KPI project outcomes. However, in cases where the model is employed to gain insights into the production rates and energy footprint over time, the presence of some of the limitations may lead to a simplified representation of the project over time.

7

Conclusions and Recommendations

7.1. Conclusions

This chapter presents the conclusion of the conducted research, where the research questions are treated to arrive at the conclusion on the main research question. To make energy-efficient strategies in the field of dredging, different techniques should be compared to optimize the fuel consumption of a maintenance dredging project. This research was conducted to facilitate the simulation of a WID and consequently compare the project results of a case study to that of a TSHD. The main research question of this study was established as:

How can a WID be effectively integrated into a method for comparing the production rates and energy footprints with conventional dredging techniques in port maintenance dredging?

To answer the main research question, this research was structured to answer the research questions initially.

1) What are the key factors and currently used methods for estimating production rates and energy footprint of a WID?

Multiple methods were treated to understand the processes of a WID during dredging. Two methods were laid out which were theoretical, two methods were empirically based formulas and a method consists of a table with factors, based on empirical data and personal experiences. It was established that two unknown parameters introduce uncertainty in the estimation, the density of the situ soil, and the entrainment factor. The density of the situ soil determines with the entrainment factor the density in the developed sediment cloud.

The key factors used for estimating the production rate were categorized into three different parameters: the soil, vessel, and hydrodynamic parameters. The soil and vessel parameters determine the excavation rate, and the hydrodynamic parameters determine how much of the fluidized material is transported to a High Energy Environment, which is the production rate of a WID. The production rate of a WID is estimated in literature by utilizing an in and out survey, but no equations or methods are present.

It was established that in this research, the direct emissions of the vessel are calculated by utilizing a bottom-up approach. This was done as over 99% of the emissions of a vessel during its life cycle are emitted during the use phase. The emissions are calculated by using mechanical or hydraulic power, a Specific Fuel Consumption factor, and a Tank To Wheel factor.

2) How can a WID be integrated into a currently available method to enable comparison of WID-based works with conventional dredging work methods?

A review of the literature revealed that simulations of dredging activities were frequently conducted in agent-based and discrete-event simulation packages, where previous research used OpenCLSim. However, OpenCLSim required adjustments to facilitate a WID due to the hydrodynamic transport method. A novel activity and accompanying processor were developed for simulating the process of a WID. The activity enabled the simulation environment to be cleared of sediments, and the developed processor was critical for the execution of the activity.

A tidal plugin was developed to simulate the working conditions under which the vessel is permitted to dredge, thereby imitating the actual operational circumstances. The production rate and emissions estimations are done by external modules, which are called by the energy plugin for each activity that is simulated. This allowed to integrate a WID in OpenCLSim and to use the energy plugin for estimating the production rate and emissions.

3) How can currently unavailable estimating modules for a WID be developed to enable comparison of WID-based work methods with conventional dredging work methods?

To estimate the energy consumption of different components onboard a WID, three modules were developed. A module simulates the power requirement needed for the propulsion, using the method proposed by Holtrop and Mennen. The power of the jet pumps was estimated by using the affinity laws, which make it possible to calculate the flow, pressure, and power requirement based on a change in pump speed. The final module estimates the power requirement of both the bow thruster and the board net appliances, which were both done by using a scaling factor and calibrated using the data extracted from the vessel logs. The modules utilize the same methodology employed in previous studies and allow to inspect the energy consumption over time. This allows to compare the results of the simulation with other dredging methods.

4) How can a WID-based work method for port maintenance be compared with conventional dredging work equipment?

To compare a WID's maintenance dredging operation, a case study in Ramsgate was selected. The case study was conducted with a WID and consequently with a TSHD. By using a case study, the site and project parameters are identical, resulting in comparable results.

It was shown that the developed method in this research allows a WID to be effectively simulated with a conventional simulation tool. This can be used to compare a WID with conventional dredging techniques for port maintenance. The developed method returns the project results such as duration and production rate, and returns the power requirement over time and the power requirement per cubic meter dredged. These KPIs allow consequently to compare different dredging techniques. The main conclusion of this research is that the developed model is now able to simulate WID's operations, visually demonstrate the power requirement during a maintenance dredging project, and compare it with other maintenance dredging equipment.

The findings of this research indicate that a WID is four times more fuel-efficient per cubic meter dredged material. One of the key reasons for this higher fuel efficiency is the operational energy distribution. The WID uses approximately 95% of its total consumed energy during the dredging phase. For a TSHD, only 70% is used during the dredging phase. This positions water injection dredging as a more sustainable and cost-effective solution for maintenance dredging operations, particularly in scenarios where energy efficiency is a primary concern.

7.2. Future research recommendations

Following the discussion of this research, recommendations to improve the model and to improve the applicability of the model are given for future research. The most significant errors in the model originated in the propeller module. As the Holtrop and Mennen yielded inaccurate results, it is recommended to investigate if the methodology can be accurately applied to smaller vessels and low sailing velocities, and additionally, how the submerged jet system affects the overall resistance of the vessel. However, it was also shown that the propeller module is not the main driver of the total power requirement, yet a new method should be constructed to improve the realism and accuracy. This was seen in the output analysis, where it was shown that, for a single dredging trip, two clear distinct clusters can be made caused by the tidal currents. This resulted in the recommendation to simulate the propulsion power with a step function, seen in Figure 7.1. However, this new method comes with limitations as the duration of a single dredging run (the width of the step function) is now a parameter that needs to be estimated. Additionally, not all dredging trips have dredging runs that are similar or perpendicular to the tidal current, increasing the difficulty of estimating the propulsion power.

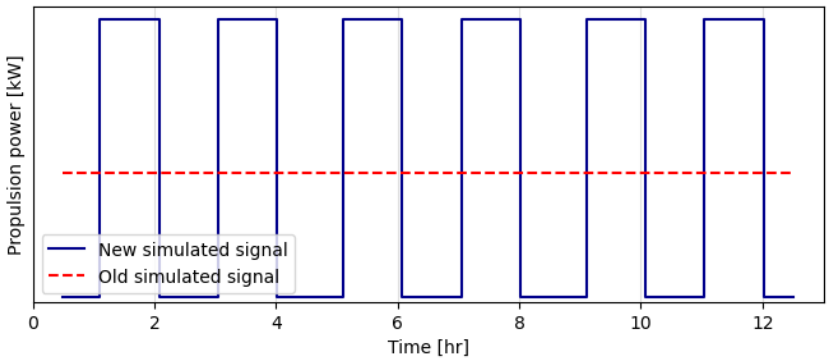

Figure 7.1: Recommended propulsion power signal (blue line) and employed propulsion power signal (red dashed line) **(Note: axis removed for confidentiality)**

It is additionally recommended that the number of case studies tested is increased, for the purpose of calibrating and validating the modules. This is only advised when the case study has sufficient and recent data, and where a WID and a TSHD have dredged, either as individual projects or as part of a joint project.

To achieve a more realistic simulation of the operational procedures of a WID, it is noted that the defined dredging sites in OpenCLSim require further attention. The dredging sites are simulated in a discrete-event simulation, thus the movement or the location of the vessel during the activity is not tracked or simulated. The dredging sites are currently modeled as a single point in space; however, as the production rate is dependent on the distance to a HEE, improvement can be made by defining the distance in space and time. This is schematized in Figure 7.2, where the dredging locations A, B, C, and D are located in the LEE and the distance to the HEE ranges between 0 and 800 meters. According to the proposed distance factors for the production rate, this can result in a deviation of 20% for the estimation. In addition, the soil conditions are not uniform for all dredging locations, so it is recommended to define multiple dredging sites, each with its own soil and hydrodynamic conditions. Preferably, a location is defined in OpenCLSim where a soil investigation has been conducted.

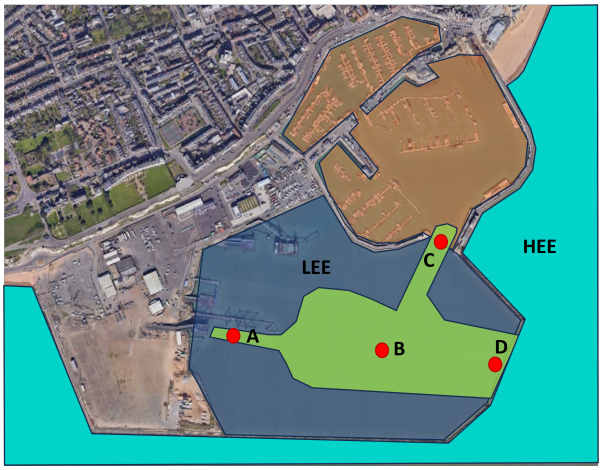

Figure 7.2: Different dredging locations (red dots) with respect to the HEE (purple area)

The model can be employed by dredging contractors to gain insight into the fuel consumption and to help with the decision-making of project parameters. It can also be employed to simulate where emissions are produced during the dredging operations, as often restrictions are present in the port. Finally, it is advised to utilize the model to determine different scenarios, if site parameters are not completely known to asses how a WID will perform under various unknown scenarios.

The outcome of the comparison made in this research showed that a WID vessel is a factor four more energy-efficient than a TSHD in the Ramsgate case study. The simulation tool and outcomes should be utilized as a guide for operational decision-making and to facilitate the adoption of a WID as a more conventional maintenance dredging method, given the increasing global focus. In addition, this model can also be used to give a deeper insight in the actuators behind the energy consumption, which components or parameters influence certain perspectives of the project.

Finally, future research should investigate the costs of the dredging operation as an additional KPI. The costs per cubic meter dredged material can further improve the decision-making for dredging contractors or port authorities in maintenance dredging operations.

References

Baart, F., Van Halem, J., & Van Koningsveld, M. (2022). OpenCLSim (v1.5.8). https://github.com/TUDelft-CITG/OpenCLSim

Bakker, F., & Van Koningsveld, M. (2023). Optimizing Bed Levels in Ports Based on Port Accessibility. *Coastal Engineering Proceedings*, (37), 62. https://doi.org/10.9753/icce.v37.papers.62

Castro, B., Mestemaker, B., & Van Den Heuvel, H. (2019). Towards Zero Emission Work Vessels: The Case of a Dredging Vessel. *Proceedings of the 2nd International Conference on Modelling and Optimisation of Ship Energy Systems*.

CEDA. (2011). Underwater Sound in Relation to Dredging. https://dredging.org/documents/ceda/html_page/2011-11_ceda_positionpaper_underwatersound_v2.pdf

CEDA. (2022). Energy Efficiency Considerations for Dredging Projects and Equipment. https://dredging.org/media/ceda/org/documents/resources/cedaonline/ceda-energy-efficient-considerations-paper.pdf

Chakraborty. (2024). *Understanding Design of Container Ships*. https://www.marineinsight.com/naval-architecture/understanding-design-of-container-ships/

Dahl, T., & Felix, C. (2020). Pump & System Curves. https://edl.pumps.org/pump-fundamentals/combined

De Boer, G., Van Halem, J., Van Koningsveld, M., Baart, F., De Niet, A., Moth, L., Klein Schaarsberg, F., & Sepehri, A. (2023). Simulating for Sustainability: Alternative Operating Strategies for Energy Efficiency. *Terra et Aqua*, (170).

De Boer, G., Van Halem, J., Hoonhout, B., Baart, F., & Van Koningsveld, M. (2022). OpenCLSim: Discrete Event Dredging Fleet Simulation to Optimise Project Costs. *WODCON XXIII*. https://www.researchgate.net/publication/360852095

Draganov, D., Ma, X., Buisman, M., Kiers, T., Heller, H., & Kirichek, A. (2021). Non-Intrusive Characterization and Monitoring of Fluid Mud: Laboratory Experiments with Seismic Techniques, Distributed Acoustic Sensing (DAS), and Distributed Temperature Sensing (DTS). In A. Manning (Ed.), *Sediment transport - recent advances*. IntechOpen. https://doi.org/10.5772/intechopen.98420

Fuller, W. P., Wagner, J., & Lewis, R. E. (2023). U.S. Hydrodynamic Dredging Challenges and Opportunities. *Transportation Research Record*, *2678*(7), 487–500. https://doi.org/10.1177/03611981231207849

Granville, P. (1976). *Elements of the Drag of Underwater Bodies* (tech. rep.). Naval Ship Research and Development Center.

Holtrop, J., & Mennen, G. G. (1982). An Approximate Power Prediction Method. *International Shipbuilding Progress*, *29*(335), 166–170.

IADC. (2013). Water Injection Dredging [Information Update]. https://www.iadc-dredging.com/wp-content/uploads/2016/07/facts-about-water-injection-dredging.pdf

IADC. (2020). Dredging Plant and Equipment [Information Update]. https://www.iadc-dredging.com/wp-content/uploads/2017/03/FA2020-02-Dredging_Plant_And_Equipment.pdf

Janssen, D. (2023). *Physics-based energy estimation during the loading phase of a TSHD* [Master's thesis, TU Delft]. https://resolver.tudelft.nl/uuid:1f4b81b4-3012-40d1-b7b1-8bff6eab766a

Kirichek, A., Cronin, K., De Wit, L., & Van Kessel, T. (2022). Advances in Maintenance of Ports and Waterways: Water Injection Dredging. In *Sediment transport - recent advances*. IntechOpen. https://doi.org/10.5772/intechopen.98750

Kirichek, A., & Rutger, R. (2020). Monitoring of Settling and Consolidation of Mud After Water Injection Dredging in the Calandkanaal. *Terra et Aqua*, 16–26.

Lamers, S. (2022). *Improved Estimations of Energy Consumption for Dredging Activities Based on Actual Data* [Master's thesis, TU Delft]. https://resolver.tudelft.nl/uuid:0a41fbed-c2e0-4441-a95b-f8dc42655be1

Matloff, N. (2008). Introduction to Discrete-Event Simulation and the Simpy Language. *Davis, CA. Dept of Computer Science*, *2*.

Merk, O. (2014). Shipping Emissions in Ports. *International Transport Forum Discussion Papers*. https://doi.org/https://doi.org/10.1787/5jrw1ktc83r1-en

Miedema, S. A. (2019). Production Estimation of Water Jets and Cutting Blades in Drag Heads. *Dredging Summit and Expo*.

Moreno-Gutiérrez, J., Calderay, F., Saborido, N., Boile, M., Rodríguez Valero, R., & Durán-Grados, V. (2015). Methodologies for Estimating Shipping Emissions and Energy Consumption: A Comparative Analysis of Current Methods. *Energy*, *86*, 603–616. https://doi.org/10.1016/j.energy.2015.04.083

Naganna, S. R., Deka, P. C., Ch, S., & Hansen, W. F. (2017). Factors Influencing Streambed Hydraulic Conductivity and Their Implications on Stream–Aquifer Interaction: A Conceptual Review. *Environmental Science and Pollution Research*, *24*(32), 24765–24789. https://doi.org/10.1007/s11356-017-0393-4

PIANC. (2014). *Harbour Approach Channels - Design Guidelines* (M. McBride, J. Briggs Michael, R. Groenveld, & M. Boll, Eds.; tech. rep.). PIANC.

Pledger, A., Johnson, M., Brewin, P., Phillips, J., Martin, S. L., & Yu, D. (2020). Characterising the Geomorphological and Physicochemical Effects of Water Injection Dredging on Estuarine Systems. *Journal of Environmental Management*, *261*, 110–259. https://doi.org/10.1016/j.jenvman.2020.110259

Prins, P. (2024). *WID thesis*. https://github.com/pepijnpp/WID_thesis.git

Rawson, K., & Tupper, E. (2001). Powering of Ships: General Principles. In *Basic ship theory* (pp. 365–410). Elsevier. https://doi.org/10.1016/B978-075065398-5/50013-3

Ribeiro da Silva, J. N., Santos, T. A., & Teixeira, A. P. (2024). Methodology for Predicting Maritime Traffic Ship Emissions Using Automatic Identification System Data. *Journal of Marine Science and Engineering*, *12*(2), 320. https://doi.org/10.3390/jmse12020320

Sadraey, M. (2009). Drag Force and Drag Coefficient. College of Engineering, Technology, and Aeronautics.

Simpson, A. R., & Marchi, A. (2013). Evaluating the Approximation of the Affinity Laws and Improving the Efficiency Estimate for Variable Speed Pumps. *Journal of Hydraulic Engineering*, *139*(12), 1314–1317. https://doi.org/10.1061/(ASCE)HY.1943-7900.0000776

Spencer, K. L., Dewhurst, R. E., & Penna, P. (2006). Potential Impacts of Water Injection Dredging on Water Quality and Ecotoxicity in Limehouse Basin, River Thames, SE England, UK. *Chemosphere*, *63*(3), 509–521. https://doi.org/10.1016/j.chemosphere.2005.08.009

Ter Meulen, G. (2018). *An Anlysis of the Draghead's Physical Processes to Determine the Trailing Forces and the Production* [Master's thesis, TU Delft].

Tyler, Z. J., Wagner, J., Schroeder, P. R., & Bailey, S. E. (2022). Water Injection Dredging: A Cost-Effective Force of Nature. *Ports 2022*, 689–697. https://doi.org/10.1061/9780784484395.068

Ujile, A. (2014). Applied Pipeline Hydraulics. In *Chemical Engineering Unit Operations, Synthesis, and Basic Design Calculations* (pp. 2–59, Vol. 1). Bomn Publishers.

Van De Ketterij, R. G., Stapersma, D., Kramers, C. H. M., & Verheijen, L. T. G. (2009). CO_2 Index: Matching the Dredging Industry's Needs With IMO. *Proceedings of the CEDA Dredging days*. https://www.researchgate.net/publication/340387122

Van Der Bilt, V. (2019). *Assessing Emission Performance of Dredging Projects* [Master's thesis, TU Delft]. https://resolver.tudelft.nl/uuid:ab6d12ea-34fe-4577-b72c-6aa688e0d1bf

Van Koningsveld, M., Verheij, H., Taneja, P., & De Vriend, H. (2021). *Ports and Waterways – Navigating the changing world*. TU Delft Open eBooks. https://doi.org/10.5074/T.2021.004

Van Koningsveld, M., Den Uijl, J., Baart, F., & Hommelberg, A. (2019). *Openclsim documentation*. Read the Docs. https://openclsim.readthedocs.io/en/latest/index.html

Van Oord. (2023). Water Injection Dredgers: A Brief Explanation of the Working Principles. https://www.vanoord.com/en/equipment/water-injection-dredger/

Van Rijn, L.C. (2012). Water Injection Dredging. https://www.leovanrijn-sediment.com/papers/Waterinjectiondredging.pdf

Vercruijsse, P., Pino, D. A., Visser, B., Roukema, D., Van Duursen, E., Benali, L., Den Boer, L., Deruyck, M., & Brouwer, R. (2023). Energy Efficiency Considerations for Dredging Projects and Equip-

ment [An Information Paper]. https://dredging.org/resources/ceda-publications-online/position-and-information-papers

Verhagen, H. (2000). Water Injection Dredging. *Proceedings of the 2nd International Conference Port Development and Coastal Environment*. https://www.researchgate.net/publication/254906604

Wasim, J., & Nine, A. H. J. (2017). Challenges in Developing a Sustainable Dredging Strategy. *Procedia Engineering*, *194*, 394–400. https://doi.org/10.1016/j.proeng.2017.08.162

Winterwerp, J. C., Wang, Z. B., Van Rester, J. A. M., & Verweij, J. F. (2002). Far-field Impact of Water Injection Dredging in the Crouch River. *Maritime Engineering*, *154*(4), 285–296. https://doi.org/10.1680/maen.154.4.285.38905

Zeng, Q., Hekkenberg, R., & Thill, C. (2019). On the Viscous Resistance of Ships Sailing in Shallow Water. *Ocean Engineering*, *190*. https://doi.org/10.1016/j.oceaneng.2019.106434

List of Figures

List of Tables

A

Propulsion power methods

A.1. Energy Efficiency Design Index (EEDI)

The International Maritime Organization (IMO) has developed a method for estimation the energy consumption of vessel to achieve the challenges set by the European Union (EU) for Greenhouse Gasses (GHG). The EEDI represent a CO_2 index value for a vessel, where the main engine and auxiliary engine are used (Van De Ketterij et al., 2009).

$$EEDI = \frac{(\sum C_{FME} \times SFC_{ME} \times P_{ME}) + P_{AE} \times C_{AE} \times SFC_{AE}}{\text{DWT} \times V_{ref}} \tag{A.1}$$

Equation A.1 gives the formula to determine the EEDI of a vessel, where C_{FME} is the conversion factor for the main engine and C_{AE} is the conversion factor for the auxiliary engine. These are multiplied with the specific fuel consumption for the main engine and the auxiliary engine (SFC_{ME} and SFC_{AE}) and the respective power consumption of the main and auxiliary engine (P_{ME} and P_{AE}). This is consequently divided by the deadweight tonnage (DWT) and the reference velocity of the vessel to achieve the EEDI.

The EEDI represent the amount of CO_2 emitted by the vessel, yet this method has large drawbacks when applied to dredging vessels. The EEDI is defined by the DWT and the velocity of the vessel, which is problematic when applied to a cutter suction dredger (CSD), as the CSD does not move. The transportation is done by additional equipment, which cannot be accounted for with the EEDI. The EEDI focuses on the free sailing stage of a vessel, even though the other dredging stages contribute significantly to the overall emissions.

A.2. STEAM method

The Ship Traffic Emissions Assessment Model (STEAM) utilizes the a combination of bottom up and top down method. The STEAM method incorporates AIS-data to determine the speed, distance and time at sea for the energy output of the vessel. The total emissions are calculated with emissions factors (Moreno-Gutiérrez et al., 2015). The emissions are calculated in Equation A.2, where i, j, k represent the emission type, engine type and fuel type. The power is represented by P in kW. The operating time T and the load factor LF are extracted from AIS-data.

$$Emissions = \sum P_j \times LF_{\text{j,l}} \times T_{\text{j,k,l}} \times EF_{\text{i,j,k}} \tag{A.2}$$

The STEAM method is considered to be more accurate then the EEDI method, as a connection between the velocity and power is made. This method can only be applied for constant velocities, as (de)accelerating is not taken into account.